

CONTHUTCH++: STOCHASTIC TRACE ESTIMATION FOR IMPLICIT INTEGRAL OPERATORS*

JENNIFER ZVONEK[†], ANDREW HORNING[‡], AND ALEX TOWNSEND[§]

Abstract. Hutchinson’s estimator is a randomized algorithm that computes an ϵ -approximation to the trace of any positive semidefinite matrix using $\mathcal{O}(1/\epsilon^2)$ matrix-vector products. An improvement of Hutchinson’s estimator, known as Hutch++, only requires $\mathcal{O}(1/\epsilon)$ matrix-vector products. In this paper, we propose a generalization of Hutch++, which we call ContHutch++, that uses operator-function products to efficiently estimate the trace of any trace-class integral operator. Our ContHutch++ estimates avoid spectral artifacts introduced by discretization and are accompanied by rigorous high-probability error bounds. We use ContHutch++ to derive a new high-order accurate algorithm for quantum density-of-states and also show how it can estimate electromagnetic fields induced by incoherent sources.

Key words. Hutchinson’s estimator, trace, integral operator, Green’s functions, density of states

AMS subject classifications. 15A15, 47G10, 68W20

1. Introduction. Estimating the trace of a matrix from matrix-vector products is a foundational task in computational mathematics. This so-called *matrix-free trace estimation* problem plays a crucial role in state-of-the-art techniques for log-determinants, eigenvalue counts, spectral densities, quantum correlations, and centrality measures on graphs [28, 8, 18, 17, 29, 19, 23, 22, 30]. In a typical application, a large matrix can be multiplied with vectors efficiently, but the diagonal entries of the matrix cannot be computed explicitly [28]. Instead, matrix-vector products with random probe vectors are used to estimate the trace with high probability. Structure in the matrix can often be leveraged to reduce the variance of these estimates [13, 15, 5, 12], and asymptotically optimal variance reduction strategies have been proposed and analyzed for symmetric positive-definite matrices [19, 21].

In many applications, the matrix-free trace estimation problem is derived by discretizing a continuous problem. The trace of the resulting matrix approximates the trace of an infinite-dimensional operator. That is, given a trace-class operator $F : L^2(\Omega) \rightarrow L^2(\Omega)$ on domain $\Omega \subset \mathbb{R}^d$ with kernel $f : \Omega \times \Omega \rightarrow \mathbb{R}$, one wants to compute the trace¹ (we use $\text{tr}(F)$ and $\text{tr}(f)$ interchangeably throughout this paper):

$$\text{tr}(F) = \int_{\Omega} f(x, x) dx < \infty.$$

The kernel $f(x, y)$ is usually not known explicitly but rather the operator-function product, defined by

$$(1.1) \quad u(x) \mapsto [Fu](x) = \int_{\Omega} f(x, y) u(y) dy, \quad \text{for a.e. } x \in \Omega,$$

can be evaluated with $u \in L^2(\Omega)$. For example, $f(x, y)$ might be a Green’s function associated with a differential operator, and evaluating (1.1) involves solving a differential equation with right-hand side u (see the examples in subsection 6.1 and subsection 6.2).

In this paper, we propose a new randomized trace estimator that uses $m \geq 1$ operator-function products to approximate the trace of F directly and achieves a specified error tolerance $\epsilon > 0$ with probability $1 - \delta > 0$. Our estimator is *discretization-oblivious*, meaning it does not depend on a particular discretization scheme to apply the operator F to functions. Instead, our algorithms and analysis are consistent with any method for (approximately) evaluating the map $u \rightarrow Fu$ on a finite set of carefully constructed smooth random functions (see subsection 3.1) and inner products in $L^2(\Omega)$. By focusing on the operator, our method holds three significant advantages over methods that work directly with discretizations of the operator:

- Our approximations converge to $\text{tr}(F)$ in expectation, and rigorous error bounds with high probability guarantees are derived. We do not require uniform spectral approximation properties of the underlying discretizations, mitigating the impact of discretization-induced spectral artifacts such as non-converged eigenvalues, spectral pollution, and spectral invisibility.

*Funding: This work is supported by National Science Foundation grant No. DMS-2045646. The work was also supported by the SciAI Center, and funded by the Office of Naval Research (ONR), under Grant Number N00014-23-1-2729.

[†]Center for Applied Mathematics, Cornell University, Ithaca, NY 14853-4201, United States (jez34@cornell.edu),

[‡]Department of Mathematics, MIT, Cambridge, MA 02142, United States (horninga@mit.edu),

[§]Mathematics Department, Cornell University, Ithaca, NY 14853-4201, United States (townsend@cornell.edu).

¹Every trace class operator can be associated with a Hilbert–Schmidt kernel that is integrable along its diagonal [4].

- Our bounds reveal explicit relationships between the accuracy of the randomized estimator and the intrinsic properties of the kernel, $f(x, y)$, such as regularity (see [section 4](#)).
- Any discretization method can be used for any trace-class kernel. Thus, optimal estimation rates for symmetric positive kernels apply even when sparse, nonsymmetric spectral methods are used for the fast and accurate solution of differential equations when evaluating $u \rightarrow Fu$.

Our approach to the operator-free trace estimator is based on a continuous analogue of the matrix-free trace estimator known as Hutch++, which interpolates between Hutchinson’s estimator and a randomized SVD estimator in a simple but asymptotically optimal way. [Section 2](#) introduces Hutchinson’s estimator, the randomized range-finder, and Hutch++ for matrices. In [section 3](#), we construct a continuous analogue of Hutchinson’s estimator and Hutch++ and present key results on their accuracy and efficiency. Error bounds for the continuous analogue of Hutchinson’s estimator and Hutch++ are derived in [section 4](#) and [section 5](#), respectively. In [section 6](#), we propose a novel algorithm that combines continuous trace estimation with high-order smoothing kernels for fast and accurate density-of-states calculations in quantum mechanics (see [subsection 6.1](#)) and show how to apply our continuous trace estimation technique to a mean-field estimation problem inspired by photonic design (see [subsection 6.2](#)).

2. Background material. We begin by describing two algorithms for estimating the trace of a matrix: (1) Hutchinson’s estimator (see [subsection 2.1](#)) and (2) Hutch++ (see [subsection 2.3](#)). Hutch++ uses the randomized range finder (see [subsection 2.2](#)) to reduce the variance of Hutchinson’s estimator.

2.1. Hutchinson’s Estimator. Hutchinson’s estimator uses matrix-vector products with random vectors to approximate the trace of a matrix when it is infeasible to calculate the trace directly [16]. Given a matrix $A \in \mathbb{R}^{n \times n}$, Hutchinson’s estimate with m probe vectors is given by

$$H_m(A) = \frac{1}{m} \sum_{i=1}^m z_i^T A z_i,$$

where $z_i \in \mathbb{R}^n$ are independent, identically distributed (i.i.d.) random vectors [16]. Common random distributions for z_i include i.i.d. standard Gaussian or Rademacher vectors, whose components are randomly chosen as $+1$ or -1 . Since these random vectors have entries with mean 0 and variance 1, Hutchinson’s estimator has the property that $\mathbb{E}[H_m(A)] = \text{tr}(A)$. Furthermore, in the case of standard Gaussian random vectors and symmetric positive semidefinite (PSD) matrices, we can explicitly determine how many matrix-vector products are needed to accurately estimate $\text{tr}(A)$ with high probability [2, Theorem 5.2]. The relative error bound below is tight when a few eigenvalues dominate the trace of A , but overestimates the relative error when the singular values of A have slow decay [19].

THEOREM 2.1. *Let $A \in \mathbb{R}^{n \times n}$ be symmetric PSD, $\varepsilon > 0$, and $0 < \delta < 1$. Let z_1, \dots, z_m be i.i.d. standard Gaussian random vectors. Then, $|H_m(A) - \text{tr}(A)| < \varepsilon \text{tr}(A)$ with probability $\geq 1 - \delta$ if $m > 20 \log(2/\delta)/\varepsilon^2$.*

We formulate a continuous analogue of Hutchinson’s estimator for the trace of a function $f : \Omega \times \Omega \rightarrow \mathbb{R}$ in [section 3](#) and prove an analogue of [Theorem 2.1](#) in [section 4](#) (see [Corollary 4.5](#)).

2.2. Randomized Range Finder. A randomized range finder approximates the column space of a matrix $A \in \mathbb{R}^{n \times n}$ by constructing an approximate basis from matrix-vector products with random vectors (e.g. standard Gaussian vectors) [14].

Algorithm 2.1 Randomized Range Finder

Input: $A \in \mathbb{R}^{n_1 \times n_2}$, target rank k , and oversampling parameter p

Output: Matrix with orthonormal columns $Q_k \in \mathbb{R}^{n_1 \times (k+p)}$, whose range approximates the range of A

- 1: Sample a matrix $G \in \mathbb{R}^{n_2 \times (k+p)}$ with i.i.d. entries drawn from a standard Gaussian distribution.
 - 2: Compute $Y = AG$.
 - 3: Compute the QR factorization $Y = Q_k R$.
-

More precisely, given a target rank k and a small oversampling parameter p , the randomized range finder uses $k + p$ matrix-vector products to approximate the span of the dominant k singular vectors of A with high probability (see [Algorithm 2.1](#)) [14].

The randomized range finder offers another way to estimate $\text{tr}(A)$. If Q is the matrix with orthonormal columns computed with the randomized range finder in [Algorithm 2.1](#) and A is well-approximated by a rank k matrix, then $QQ^T A \approx A$. Therefore, $\text{tr}(A) \approx \text{tr}(QQ^T A) = \text{tr}(Q^T A Q)$ by the cyclic property of trace. The matrix $Q^T A Q$ is of size $(k+p) \times (k+p)$, which is typically much smaller than A itself. This technique is particularly effective when the singular values of A decay rapidly.

2.3. Hutch++. Since Hutchinson’s estimator and the randomized range finder are most effective in complimentary circumstances, they can be combined to obtain an improved estimate for the trace of a matrix. Hutch++ does this by splitting a symmetric PSD matrix A into two terms: (1) $QQ^T A QQ^T$ and (2) $A - QQ^T A QQ^T$, where Q is the orthonormal output of the randomized range finder in [Algorithm 2.1](#) [19]. The trace of $QQ^T A QQ^T$ is computed exactly while the trace of $A - QQ^T A QQ^T$ is computed using Hutchinson’s estimator. The result is an estimator that uses only $\mathcal{O}(1/\varepsilon)$ matrix-vector products to estimate $\text{tr}(A)$ to within a relative error bound of ε (see [Algorithm 2.2](#)). In particular,

Algorithm 2.2 Hutch++

Input: Matrix-vector products from a symmetric PSD matrix $A \in \mathbb{R}^{n \times n}$ and the number of queries m .

Output: Estimate of $\text{tr}(A)$.

- 1: Sample two random matrices, $S \in \mathbb{R}^{n \times m/3}$, $G \in \mathbb{R}^{n \times m/3}$, each with i.i.d. Gaussian entries.
 - 2: Compute $Y = AS$.
 - 3: Compute the QR factorization $Y = QR$.
 - 4: **Return:** $\text{Hutch++}(A) = \text{tr}(Q^T A Q) + \frac{3}{m} \text{tr}(G^T (I - QQ^T) A (I - QQ^T) G)$.
-

Hutch++ has the following probabilistic error bound [19, Theorem 1.1]:

THEOREM 2.2. *Let $\varepsilon > 0$, $0 < \delta < 1$, and $A \in \mathbb{R}^{n \times n}$ be symmetric PSD. If Hutch++ is used with $m = \mathcal{O}(\sqrt{\log(1/\delta)}/\varepsilon + \log(1/\delta))$ matrix-vector products, then with probability $\geq 1 - \delta$,*

$$|\text{Hutch++}(A) - \text{tr}(A)| \leq \varepsilon \text{tr}(A).$$

[Section 3](#) extends the Hutch++ estimator to one for continuous functions $f : \Omega \times \Omega \rightarrow \mathbb{R}$. Our algorithm follows the same general steps, but some added complications result from using functions instead of matrices. However, we obtain the same asymptotic bound of $\mathcal{O}(\sqrt{\log(1/\delta)}/\varepsilon + \log(1/\delta))$ (see [Corollary 5.3](#) in [section 5](#)) for the required number of operator-function products of the form [\(1.1\)](#).

3. Trace Estimation for Functions. This section introduces the algorithms and corresponding error bounds for a continuous version of Hutchinson’s estimator (see [subsection 3.3](#)) and ContHutch++ (see [subsection 3.4](#)). We defer the analysis of these estimators to [section 4](#) and [section 5](#), respectively, and focus on the algorithms and results here. To develop continuous versions of Hutchinson’s estimator and Hutch++, we must first establish continuous versions of the mechanics used for the discrete estimators. We describe Gaussian processes, which are the continuous analogues of random vectors, in [subsection 3.1](#) and quasimatrices, which are continuous analogues of matrices, in [subsection 3.2](#).

3.1. Gaussian Processes. A function, g , drawn from a Gaussian process (GP) is an infinite dimensional analogue of a vector drawn from a multivariate Gaussian distribution in the sense that samples from g follow a multivariate Gaussian distribution. More precisely, we write $g \sim \mathcal{GP}(0, K)$ for some continuous positive definite kernel $K : \Omega \times \Omega \rightarrow \mathbb{R}$ if for any $x_1, \dots, x_n \in \Omega$, $(g(x_1), \dots, g(x_n))$ follows a multivariate Gaussian distribution with mean $(0, \dots, 0)$ and covariance $K_{ij} = K(x_i, x_j)$ for $1 \leq i, j \leq n$.

We are particularly interested in the squared exponential covariance kernel

$$K_{SE}(x, y) = \frac{1}{\ell \sqrt{2\pi}} \exp\left(-\frac{(x - y)^2}{2\ell^2}\right),$$

where $s_\ell = \ell \sqrt{2\pi}$ is a scaling factor chosen such that $\int_{\mathbb{R}} K_{SE}(0, y) dy = \int_{\mathbb{R}} \frac{1}{s_\ell} e^{-y^2/(2\ell^2)} dy = 1$. The length scale parameter ℓ determines how correlated samples of g are. If ℓ is large, then the samples $g(x_1), \dots, g(x_n)$ are highly correlated and g is close to a constant function. If ℓ is small, then samples of g are only weakly correlated and g is usually a highly oscillatory function. The algorithms in this

paper can be used for any symmetric positive definite kernel. However, we present our results in terms of the squared exponential kernel to obtain specific bounds in terms of the length scale parameter ℓ .

Note that GPs produce continuous functions. Thus, if g is drawn from $\mathcal{GP}(0, K)$, then there is a positive correlation between $g(x)$ and $g(y)$. This contrasts with the random vectors that are commonly used in Hutchinson’s estimator and Hutch++, which have independent entries. Thus, our estimates have some extra quantities to account for this positive correlation.

3.2. Quasimatrices. Quasimatrices are an infinite dimensional analogue of tall-skinny matrices [26]. Let $\Omega_1, \Omega_2 \subseteq \mathbb{R}$ be two domains and denote by $L^2(\Omega_1)$ the space of square-integrable functions defined on Ω_1 . Many of the results in this paper are easier to state using quasimatrices. We say that \mathbf{B} is an $\Omega_1 \times k$ quasimatrix, if \mathbf{B} is a matrix with k columns where each column is a function defined on Ω_1 . That is,

$$\mathbf{B} = [b_1 \mid \cdots \mid b_k], \quad b_j : \Omega_1 \rightarrow \mathbb{R}.$$

Throughout this paper, we assume that the columns of B are square-integrable (i.e., $b_j \in L^2(\Omega_1)$).

Quasimatrices are useful for defining analogues of matrix operations for Hilbert–Schmidt (HS) operators [9, 25, 26, 27]. For example, if $F : L^2(\Omega_1) \rightarrow L^2(\Omega_2)$ is a HS operator, then we write $F\mathbf{B}$ to denote the quasimatrix obtained by applying F to each column of \mathbf{B} . Moreover, we write $\mathbf{B}^*\mathbf{B}$ and $\mathbf{B}\mathbf{B}^*$ to mean the following:

$$\mathbf{B}^*\mathbf{B} = \begin{bmatrix} \langle b_1, b_1 \rangle & \cdots & \langle b_1, b_k \rangle \\ \vdots & \ddots & \vdots \\ \langle b_k, b_1 \rangle & \cdots & \langle b_k, b_k \rangle \end{bmatrix}, \quad \mathbf{B}\mathbf{B}^* = \sum_{j=1}^k b_j(x)b_j(y),$$

where $\langle \cdot, \cdot \rangle$ is the $L^2(\Omega_1)$ inner-product. A quasimatrix Q has orthonormal columns if Q^*Q is the identity matrix. Many operations for rectangular matrices in linear algebra, such as the QR factorization, can be generalized to quasimatrices [26].

3.3. Continuous Hutchinson’s Estimator. We now extend Hutchinson’s estimator to trace estimation of continuous functions $f : \Omega \times \Omega \rightarrow \mathbb{R}$, where $\Omega = [a, b]$ is an interval in \mathbb{R} with $-\infty < a < b < \infty$. That is, we want to approximate $\text{tr}(f) = \int_{\Omega} f(x, x)dx$. In the discrete case, Hutchinson’s estimator can use i.i.d. standard Gaussian vectors to approximate $\text{tr}(A)$. Thus, we propose using functions drawn from a GP to estimate the trace of a function. We propose the estimator

$$(3.1) \quad H_m(f) = \frac{1}{m} \sum_{i=1}^m \int_{\Omega} \int_{\Omega} g_i(x)f(x, y)g_i(y)dx dy,$$

where each g_i is independently drawn from $\mathcal{GP}(0, K)$. We can express the estimator in (3.1) in terms of quasimatrices. Let F be the integral operator corresponding to the function $f \in L^2(\Omega \times \Omega)$ such that $(Fg)(x) = \int_{\Omega} f(x, y)g(y)dy$ for all $g \in L^2(\Omega)$ and $x \in \Omega$. Then, if G is the $\Omega \times m$ quasimatrix whose i th column is g_i , we can rewrite the continuous Hutchinson’s estimator as

$$(3.2) \quad H_m(f) = \frac{1}{m} \sum_{i=1}^m [G^*(FG)]_{ii} = \frac{1}{m} \text{tr}(G^*(FG)),$$

where the operator-function product FG must be computed before applying G^* from the left. Written in this form, we see that the continuous Hutchinson’s estimator takes the same form as the discrete Hutchinson’s estimator, except here, FG requires integration instead of matrix-vector products.

It can be shown that the continuous Hutchinson’s estimator in (3.2) converges to $\text{tr}(f)$ as $\ell \rightarrow 0$. For a fixed $\ell > 0$, note that $\mathbb{E}[H_m(f)]$ is not precisely $\text{tr}(f)$ because of the covariance kernel K in the Gaussian process used to generate the functions g_i . However, as $\ell \rightarrow 0$, we find that $\mathbb{E}[H_m(f)] \rightarrow \text{tr}(f)$ (see Corollary 4.5). In particular, if f is Lipschitz continuous and the squared exponential kernel is used with parameter $\ell = \mathcal{O}(\varepsilon/\sqrt{\log(1/\varepsilon)})$ then we have $|\mathbb{E}[H_m(f)] - \text{tr}(f)| < \varepsilon$. Furthermore, if $m = \mathcal{O}(\log(1/\delta)/\varepsilon^2)$ operator-function products are used, then $\mathbb{P}[|H_m(f) - \text{tr}(f)| \geq \varepsilon \|f\|_{L^2}] \leq \delta$ (see Theorem 4.4). For PSD functions, we have that $\|f\|_{L^2} \leq \text{tr}(f)$ so that we may write this bound in terms of $\text{tr}(f)$ to obtain a relative error bound.

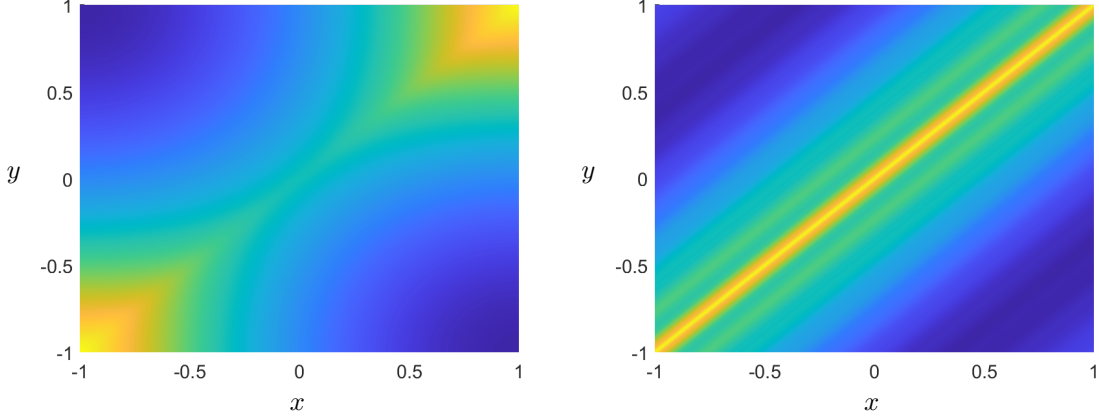


Fig. 3.1: Two symmetric positive definite kernels are used for trace estimation experiments: the Helmholtz-like kernel in (3.3) (left panel) and the combination of sinc kernels in (3.4) (right panel).

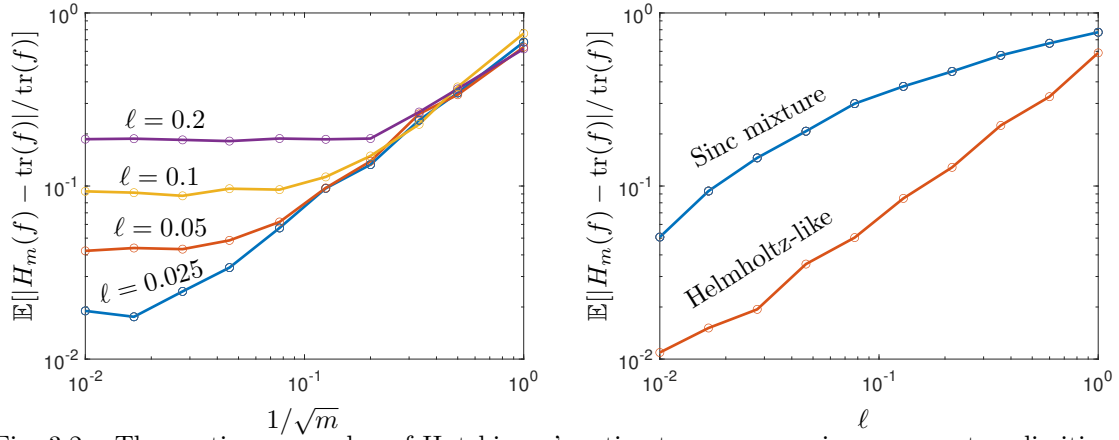


Fig. 3.2: The continuous analog of Hutchinson’s estimator converges in mean up to a limiting bias determined by the covariance parameter $\ell > 0$ for the Gaussian process, as demonstrated for the Helmholtz-like kernel in (3.3) (left panel). This limiting bias decreases at a controlled rate as $\ell \rightarrow 0$ when m is selected adaptively to balance the sample error and covariance error (right panel). The precise rate of decrease depends on the kernel’s modulus of continuity (see Theorem 4.1).

To demonstrate the convergence of the continuous Hutchinson’s estimator, we tested the estimator on two functions: a Helmholtz-like function (left panel of Figure 3.1)

$$(3.3) \quad f(x, y) = \left(1 - \cos\left(\frac{\pi(x+1)}{4}\right)\right) \sin\left(\frac{\pi(y+1)}{4}\right) + \frac{1}{1 + e^{5(x-y)}} \left(1 - \cos\left(\frac{\pi(y+1)}{4}\right) \sin\left(\frac{\pi(x+1)}{4}\right)\right),$$

and a combination of three sinc functions (right panel of Figure 3.1)

$$(3.4) \quad f(x, y) = \text{sinc}(x - y) + \frac{1}{2} \text{sinc}(10(x - y)) + \frac{1}{4} \text{sinc}(50(x - y)),$$

both shown in Figure 3.1. The convergence results are shown in Figure 3.2. In the left panel, we see that the relative accuracy of the estimator for the trace of the Helmholtz-like function converges linearly in expectation with $1/\sqrt{m}$ up to some bias determined by the value of ℓ . This bias decreases as ℓ decreases. A similar trend holds for the combination of sinc functions. The right panel shows the relative accuracy of the estimator for both test functions. We see in the right panel that the trace

Algorithm 3.1 ContHutch++

Input: Operator-function products with the integral operator F associated with a continuous, symmetric, PSD function $f : \Omega \times \Omega \rightarrow \mathbb{R}$, number m of queries, and length-scale parameter ℓ .

Output: Estimate of $\text{tr}(f)$.

- 1: Sample two random $\Omega \times m/3$ quasimatrices, S and G , whose i.i.d. columns are each drawn from $\mathcal{GP}(0, K_{SE})$.
 - 2: Compute $Y = FS$.
 - 3: Compute the QR factorization $Y = QR$ to find an $\Omega \times m/3$ quasimatrix, Q , with orthonormal columns.
 - 4: **Return:** $\text{ContHutch}++(f) = \text{tr}(Q^T F Q) + \frac{3}{m} \text{tr}(\tilde{G}^T (F \tilde{G}))$, where $\tilde{G} = (I - QQ^T)G$.
-

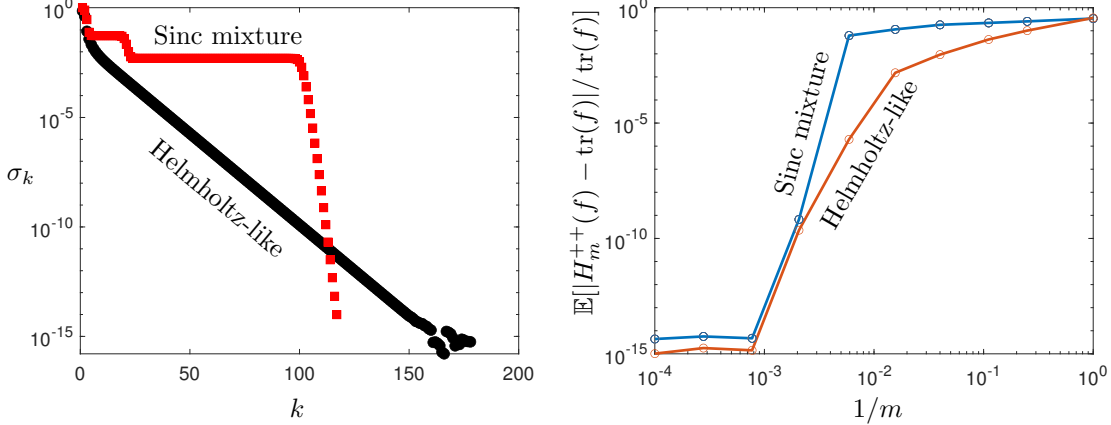


Fig. 3.3: The Hutch++ estimator leverages spectral decay to compute $\text{tr}(f)$ with high-accuracy. The spectrum of the two kernels is shown in the left panel, and the expected relative error in the trace (estimated from samples) is plotted against $1/m$ in the right panel (with $\ell = 0.05$).

estimate for both functions converges to the exact value as ℓ decreases. The exact convergence rate depends on the function’s modulus of continuity (see [Theorem 4.1](#) for more details).

3.4. ContHutch++. Just as Hutch++ uses the randomized range finder to improve on Hutchinson’s estimator, we can use the continuous randomized range finder [3] to improve on the continuous Hutchinson’s estimator for estimating the trace of a symmetric PSD function. Note that a function $f : \Omega \times \Omega \rightarrow \mathbb{R}$ is PSD if for any $x_1, \dots, x_n \in \Omega$, the matrix $A \in \mathbb{R}^{n \times n}$ with $A_{ij} = f(x_i, x_j)$ is PSD. To do so, we split the integral operator F corresponding to the function f into two terms: (1) QQ^*FQQ^* and (2) $F - QQ^*FQQ^*$, where Q is the quasimatrix computed by the continuous randomized range finder applied to F . The trace of the first term can be rewritten as the trace of a matrix and computed exactly as $\text{tr}(QQ^*FQQ^*) = \text{tr}(Q^*FQ)$. The trace of the second term is approximated using the continuous Hutchinson’s estimator (see [Algorithm 3.1](#)). Note that if F is the integral operator with continuous, symmetric PSD kernel f , then $\text{tr}(F) = \text{tr}(f)$ [4].

As in the discrete case, we achieve a bound on the number of operator-function products, which is $\mathcal{O}(\sqrt{\log(1/\delta)}/\varepsilon + \log(1/\delta))$ (see [Corollary 5.3](#)). To demonstrate this, we tested ContHutch++ on the two example functions we looked at in [subsection 3.3](#). The spectral decay of both functions is shown in the left panel of [Figure 3.3](#). The singular values of the Helmholtz-like function initially decay much faster than the singular values of the sinc mixture function. The ContHutch++ estimate converges with rate $\mathcal{O}(1/m)$ during spectral plateaus but exploits spectral decay to achieve high accuracy.

4. Analyzing the Continuous Hutchinson’s estimator. We now turn to analyzing the continuous Hutchinson’s estimator.

THEOREM 4.1. *Let $\varepsilon > 0$ and $f : \Omega \times \Omega \rightarrow \mathbb{R}$ be a continuous function, where $\Omega = [a, b]$ with $-\infty < a < b < \infty$. Let $d = d(\varepsilon)$ be such that $|f(x, y) - f(x, z)| \leq \frac{\varepsilon}{4(b-a)}$ for all $y, z \in \Omega$ such that $|y - z| < d$. If $H_m(f)$ is the continuous Hutchinson’s estimate of $\text{tr}(f)$ with kernel K_{SE} and length-scale*

parameter $\ell < \min \left\{ \frac{d}{\sqrt{2 \log(8\|f\|_\infty(b-a)/\varepsilon)}}, \frac{5\varepsilon}{26\|f\|_\infty} \right\}$, then

$$|\mathbb{E}[H_m(f)] - \text{tr}(f)| < \varepsilon,$$

where $\|f\|_\infty = \max_{x,y \in \Omega} |f(x,y)|$.

Proof. The expectation of $H_1(f)$ is

$$\mathbb{E}[H_1(f)] = \int_{\Omega} \int_{\Omega} f(x,y) \mathbb{E}[g_i(x)g_i(y)] dx dy = \int_{\Omega} \int_{\Omega} f(x,y) K_{SE}(x,y) dx dy,$$

since $K_{SE}(x,y) = \mathbb{E}[(g_i(x) - \mathbb{E}[g_i(x)])(g_i(y) - \mathbb{E}[g_i(y)])] = \mathbb{E}[g_i(x)g_i(y)]$. Thus, we find that

$$\mathbb{E}[H_m(f)] = \frac{1}{m} \sum_{i=1}^m \mathbb{E}[H_1(f)] = \mathbb{E}[H_1(f)] = \int_{\Omega} \int_{\Omega} f(x,y) \frac{1}{\ell\sqrt{2\pi}} \exp(-(x-y)^2/(2\ell^2)) dx dy.$$

Since $\int_{\mathbb{R}} K_{SE}(x,y) dy = 1$, we can write $f(x,x) = \int_{\mathbb{R}} f(x,x) K_{SE}(x,y) dy$. This means that we have,

$$\begin{aligned} |\mathbb{E}[H_m(f)] - \text{tr}(f)| &\leq \int_{\Omega} \left| \int_{\Omega} f(x,y) K_{SE}(x,y) dy - f(x,x) \right| dx \\ (4.1) \quad &\leq \underbrace{\int_{\Omega} \left| \int_{\Omega} (f(x,y) - f(x,x)) K_{SE}(x,y) dy \right| dx}_{I_1} + \underbrace{\int_{\Omega} \left| \int_{\mathbb{R} \setminus \Omega} f(x,x) K_{SE}(x,y) dy \right| dx}_{I_2}. \end{aligned}$$

We will show that $I_1 \leq \varepsilon/2$ and $I_2 \leq \varepsilon/2$ so that $|\mathbb{E}[H_m(f)] - \text{tr}(f)| \leq \varepsilon$. To evaluate I_1 in (4.1), we partition the domain of integration $\Omega \times \Omega$ into $\Omega \times \{y : |x-y| < d\}$ and $\Omega \times \{y : |x-y| \geq d\}$. We also use the fact that $|f(x,y) - f(x,x)| < \varepsilon/(4(b-a))$ when $|x-y| < d$ to simplify the inner integral in I_1 to

$$\begin{aligned} I_1 &\leq \frac{1}{\ell\sqrt{2\pi}} \int_{\Omega} \int_{|x-y| < d} \frac{\varepsilon}{4(b-a)} \exp(-(x-y)^2/(2\ell^2)) dy dx \\ &\quad + \frac{1}{\ell\sqrt{2\pi}} \int_{\Omega} \int_{|x-y| \geq d} |f(x,y) - f(x,x)| \exp(-(x-y)^2/(2\ell^2)) dy dx. \end{aligned}$$

Since $\int_{|x-y| < d} K_{SE}(x,y) dy \leq \int_{\mathbb{R}} K_{SE}(x,y) dy = 1$ and $|f(x,y) - f(x,x)| \leq |f(x,y)| + |f(x,x)| \leq 2\|f\|_\infty$, we have

$$I_1 \leq \int_{\Omega} \frac{\varepsilon}{4(b-a)} dx + \frac{2\|f\|_\infty}{\ell\sqrt{2\pi}} \int_{\Omega} \int_{|x-y| \geq d} \exp(-(x-y)^2/(2\ell^2)) dy dx.$$

By evaluating the first term exactly and bounding the second term, we find that

$$\begin{aligned} I_1 &\leq \frac{\varepsilon}{4} + 2\|f\|_\infty(b-a) \left(1 - \text{erf} \left(\frac{d}{\ell\sqrt{2}} \right) \right) \\ &\leq \frac{\varepsilon}{4} + 2\|f\|_\infty(b-a) \exp \left(-\frac{d^2}{2\ell^2} \right), \end{aligned}$$

where erf denotes the error function, and the second inequality comes from the fact that $1 - \text{erf}(x) \leq \exp(-x^2)$ for $x > 0$. Thus, we have that $I_1 \leq \varepsilon/2$ since $\ell < d/\sqrt{2 \log(8\|f\|_\infty(b-a)/\varepsilon)}$.

To bound I_2 in (4.1), we partition the domain of integration $\Omega \times (\mathbb{R} \setminus \Omega)$ into three pieces D_1 , D_2 , and D_3 such that $\Omega \times (\mathbb{R} \setminus \Omega) = D_1 \cup D_2 \cup D_3$:

$$\begin{aligned} D_1 &= \left([a, a + \ell\sqrt{2}] \times [a - \ell\sqrt{2}, a] \right) \cup \left([b - \ell\sqrt{2}, b] \times [b, b + \ell\sqrt{2}] \right), \\ D_2 &= \left((a + \ell\sqrt{2}, b] \times [a - \ell\sqrt{2}, a] \right) \cup \left([a, b - \ell\sqrt{2}] \times [b, b + \ell\sqrt{2}] \right), \\ D_3 &= \left([a, b] \times (-\infty, a - \ell\sqrt{2}) \right) \cup \left([a, b] \times (b + \ell\sqrt{2}, \infty) \right). \end{aligned}$$

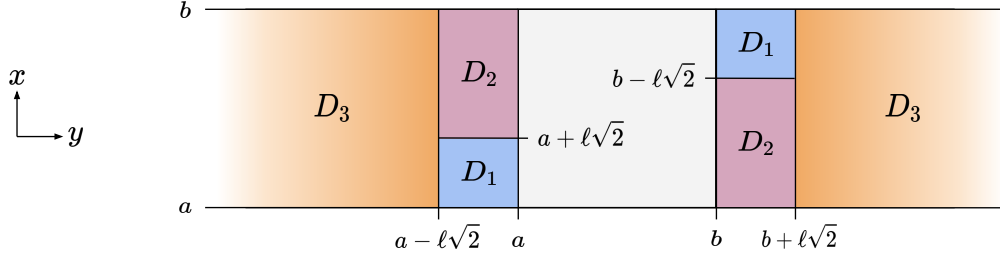


Fig. 4.1: Domains of integration for computing the second term in (4.1).

See Figure 4.1 for a depiction of these three domains. On D_1 , we use the fact that $f(x, x) \leq \|f\|_\infty$ for all $x \in \Omega$ and that $K_{SE}(x, y) \leq 1/\ell\sqrt{2\pi}$ to obtain a bound of $2\ell\sqrt{2/\pi}\|f\|_\infty$. In domains D_2 and D_3 , we know that $|x - y|/(\ell\sqrt{2}) \geq 1$, so we have that $\exp(-(x - y)^2/(2\ell^2)) \leq \exp(-|x - y|/(\ell\sqrt{2}))$. Using this bound, we can evaluate the integral over D_2 directly to get a bound of $2\sqrt{2/\pi}\ell\|f\|_\infty(e^{-1} - e^{-2} - e^{-(b-a)/(\ell\sqrt{2})} + e^{-(b-a+\ell\sqrt{2})/(\ell\sqrt{2})})$. Similarly, bounding the integral over D_3 gives a bound of $2\sqrt{2/\pi}\ell\|f\|_\infty(e^{-1} - e^{-(b-a+\ell\sqrt{2})/(\ell\sqrt{2})})$. Combining our three error bounds, we find that

$$\begin{aligned} \int_{\Omega} \left| \int_{\mathbb{R} \setminus \Omega} f(x, x) K_{SE}(x, y) dy \right| dx &\leq 2\sqrt{\frac{2}{\pi}} \left(1 + 2e^{-1} - e^{-2} - e^{-(b-a)/(\ell\sqrt{2})}\right) \ell \|f\|_\infty \\ &\leq 2\sqrt{\frac{2}{\pi}} (1 + 2e^{-1} - e^{-2}) \ell \|f\|_\infty \\ &\leq \frac{13}{5} \ell \|f\|_\infty \leq \varepsilon/2 \end{aligned}$$

where the last inequality follows from $\ell < 5\varepsilon/(26\|f\|_\infty)$. \square

Thus, the length-scale parameter determines how close the expected value of our estimate is to the correct trace. Note that d depends on ε , so we need $\ell = \mathcal{O}\left(\min\left\{d/\sqrt{\log(1/\varepsilon)}, \varepsilon\right\}\right)$. However, if f is Lipschitz with Lipschitz constant α in the second variable, then we have that $d = \varepsilon/\alpha$, so ℓ scales with $\varepsilon/\sqrt{\log(1/\varepsilon)}$ to achieve $|\mathbb{E}[H_m(f)] - \text{tr}(f)| < \varepsilon$. Similarly, other forms of continuity, such as Hölder continuity, give different relationships between ℓ and ε .

Next, we use the Hanson–Wright inequality to show that the number of operator-function products m determines the probability that the continuous Hutchinson’s estimate is close to $\text{tr}(f)$.

4.1. Hanson–Wright inequality. The Hanson–Wright inequality is a result in probability theory that gives an upper bound on the tail probability of a sum of independent, mean-zero random variables with bounded variances. Specifically, it states that if X_1, \dots, X_n are independent, mean-zero random variables with variances bounded by b_i^2 (i.e., $\mathbb{E}[X_i^2] \leq b_i^2$), and $\epsilon > 0$, then for any $t > 0$,

$$\mathbb{P}\left(\left|\sum_{i=1}^n X_i\right| \geq t\right) \leq C \exp\left(-\frac{ct^2}{\sum_{i=1}^n b_i^2 + \epsilon t}\right),$$

where C and c are positive constants. The inequality is beneficial for analyzing the behavior of random matrices and is often used in high-dimensional statistics and machine learning. In the context of Hutchinson’s estimator, it is used to show that Hutchinson’s estimate is accurate with exceptionally high probability [19]. We present a continuous version of the Hanson–Wright inequality to obtain a similar high-probability result.

The following theorem tells us that if f is a symmetric PSD function, we can bound the probability that the continuous Hutchinson’s estimate is far from its expected value. To do so, we define the operator $\phi : L^2(\Omega) \rightarrow \mathbb{R}$ in terms of f such that $\phi(g)$ is the continuous Hutchinson’s estimate of $\text{tr}(f)$ with $m = 1$. We first show that $\phi(g)$ is close to its expected value with high probability, then in subsection 4.2 we use this result to show that the full continuous Hutchinson’s estimate is close to $\text{tr}(f)$ with high probability.

THEOREM 4.2. Let $g \sim \mathcal{GP}(0, K_{SE})$ and $f : \Omega \times \Omega \rightarrow \mathbb{R}$ be a symmetric, PSD, continuous function, where $\Omega = [a, b]$ with $-\infty < a < b < \infty$. Define $\phi(g) = \int_{\Omega} \int_{\Omega} g(x) f(x, y) g(y) dx dy$. Then, we have

$$\mathbb{P}(|\phi(g) - \mathbb{E}[\phi(g)]| \geq t) \leq 27 \exp\left(-\frac{1}{C} \min\left(\frac{t^2}{\|f\|_{L^2}^2 \|K_{SE}\|_{op}}, \frac{t}{\|f\|_{op}}\right)\right), \quad t > 0,$$

where C can be taken as $\max\{64, 54^2 8^4 / \|K_{SE}\|_{op}\}$.²

Proof. See [Appendix A](#). □

A similar result to [Theorem 4.2](#) holds for all continuous functions that can be decomposed as $f = f_1 - f_2$, where f_1, f_2 are continuous PSD functions in $L^2(\Omega \times \Omega)$, with the same assumptions as in [Theorem 4.2](#).

COROLLARY 4.3. Let $f : \Omega \times \Omega \rightarrow \mathbb{R}$ be any continuous function that can be written as $f = f_1 - f_2$, for continuous PSD functions f_1, f_2 in $L^2(\Omega \times \Omega)$. Then,

$$\mathbb{P}(|\phi(g) - \mathbb{E}[\phi(g)]| \geq t) \leq 54 \exp\left(-\frac{1}{C} \min\left\{\frac{t^2}{4\|f\|_{L^2}^2 \|K_{SE}\|_{op}}, \frac{t}{2\|f\|_{op}}\right\}\right),$$

where C can be taken as $\max\{64, 54^2 8^4 / \|K_{SE}\|_{op}\}$.

Proof. See [Appendix A](#). □

In many cases, f can be decomposed as $f = f_1 - f_2$ as required for [Corollary 4.3](#). Note that defining ϕ in terms of a continuous function f is the same as defining ϕ in terms of the symmetric function $\tilde{f}(x, y) = \frac{1}{2}(f(x, y) + f(y, x))$. Thus, we can treat f as symmetric for the following argument. When $f : \Omega \times \Omega \rightarrow \mathbb{R}$ is continuous and symmetric, the integral operator F defined by $(Fg)(x) = \int_{\Omega} f(x, y) g(y) dy$ for $x \in \Omega$ is self-adjoint and compact. This means we can write down an orthonormal basis of eigenfunctions e_1, e_2, \dots and eigenvalues $\lambda_1, \lambda_2, \dots$ such that $F e_j = \lambda_j e_j$, where equality holds in the L^2 sense. For eigenfunctions corresponding to nonzero eigenvalues, e_j is a continuous function (by the same reasoning as in the proof of Mercer's Theorem). If there are a finite number of positive eigenvalues or a finite number of negative eigenvalues, then we can write f as $f = f_1 - f_2$, where equality holds in the L^2 sense. Let $S = \{i : \lambda_i \geq 0\}$. Then f_1 and f_2 are given by $f_1(x, y) = \sum_{i \in S} \lambda_i e_i(x) e_i(y)$ and $f_2(x, y) = -\sum_{j \in \mathbb{N} \setminus S} \lambda_j e_j(x) e_j(y)$, which gives two PSD functions.

If F has an infinite number of positive and negative eigenvalues, we cannot choose such a decomposition for f_1 and f_2 . However, if f is Lipschitz continuous, then the eigendecomposition of f is absolutely convergent [\[24\]](#) and we can decompose f into two PSD functions as we did for the case of finitely many positive or negative eigenvalues. In practice, there are many Green's functions that do not have an infinite number of both positive and negative eigenvalues. For example, Green's functions corresponding to uniformly self-adjoint elliptic partial differential equations have infinitely many positive eigenvalues but, at most, a finite number of negative eigenvalues.

4.2. An Error Bound for the Continuous Hutchinson's Estimator. We now use our continuous Hanson–Wright inequality to prove that the continuous Hutchinson's estimator is accurate with exceptionally high probability.

THEOREM 4.4. Let $0 < \delta < 1$ and $f : \Omega \times \Omega \rightarrow \mathbb{R}$ be a continuous function with $\Omega = [a, b]$ and $-\infty < a < b < \infty$, where f can be written as $f = f_1 - f_2$ for some continuous PSD functions $f_1, f_2 : \Omega \times \Omega \rightarrow \mathbb{R}$. Let $m \geq \frac{\log(54/\delta)}{4C\|K_{SE}\|_{op}}$. Then, with probability $\geq 1 - \delta$,

$$|H_m(f) - \mathbb{E}[H_m(f)]| \leq 2\|f\|_{L^2} \sqrt{\frac{C \log(54/\delta) \|K_{SE}\|_{op}}{m}}, \quad C = \max\{64, 54^2 8^4 / \|K_{SE}\|_{op}\},$$

where $H_m(f)$ is the continuous Hutchinson's estimate of $\text{tr}(f)$ with m probe functions drawn from $\mathcal{GP}(0, K_{SE})$.

Proof. We first define new functions, \bar{f} and \bar{g} , defined by block repetitions of f and g , respectively. This will allow us to use the continuous Hanson–Wright inequality (see [Corollary 4.3](#)) to bound the failure probability of the continuous Hutchinson's estimate of $\text{tr}(f)$ with m probe functions. To do

²In practice, C is much smaller than the bound provided, and we expect that a smaller bound could be found. See [\[11\]](#), for example.

so, define the intervals $\Omega_i = [a + i(b - a), a + (i + 1)(b - a))$ for $0 \leq i \leq m - 2$ and $\Omega_{m-1} = [a + (m-1)(b-a), a + m(b-a)]$. Define the union of these domains as $\bar{\Omega} = \bigcup_{i=0}^{m-1} \Omega_i = [a, m(b-a) + a]$. Then, since the Ω_i 's are disjoint, for any $x \in \bar{\Omega}$, there exists a unique $0 \leq i \leq m - 1$ such that $x \in \Omega_i$. Thus, we define our block extension of f to be $\bar{f} : \bar{\Omega} \times \bar{\Omega} \rightarrow \mathbb{R}$ such that

$$\bar{f}(x, y) = \begin{cases} f(x - i(b - a), y - i(b - a)), & \text{if } x, y \in \Omega_i, \\ 0, & \text{otherwise.} \end{cases}$$

Similarly, if g_0, \dots, g_{m-1} are i.i.d. functions drawn from $\mathcal{GP}(0, K_{SE})$, we define $\bar{g} : \bar{\Omega} \rightarrow \mathbb{R}$ by

$$\bar{g}(x) = g_i(x - i(b - a)), \quad x \in \Omega_i.$$

Note that \bar{g} then has the covariance kernel $\bar{K}_{SE} : \bar{\Omega} \times \bar{\Omega} \rightarrow \mathbb{R}$, which is defined as a block extension of the covariance kernel K_{SE} in the same way that \bar{f} is defined in terms of f .

We can then rewrite the continuous Hutchinson's estimator in terms of \bar{f} and \bar{g} so that

$$\frac{1}{m} \sum_{i=1}^m \int_{\Omega} \int_{\Omega} g_i(x) f(x, y) g_i(y) dx dy = \frac{1}{m} \int_{\bar{\Omega}} \int_{\bar{\Omega}} \bar{g}(x) \bar{f}(x, y) \bar{g}(y) dx dy.$$

Note that \bar{f} is only a continuous function if f is zero on the boundary of Ω . However, the reason that [Corollary 4.3](#) requires continuity is to apply Mercer's theorem to find an eigendecomposition of f . Since f is continuous on Ω and \bar{f} is formed from blocks of f , we can still apply Mercer's theorem to f and then form \bar{f} by zero-extending the eigenfunctions of f appropriately. Thus, we can use the Hanson-Wright inequality even though \bar{f} is discontinuous. [Corollary 4.3](#) tells us that

$$(4.2) \quad \mathbb{P}(|\phi_{\bar{f}}(\bar{g}) - \mathbb{E}[\phi_{\bar{f}}(\bar{g})]| \geq t) \leq 54 \exp\left(-\frac{1}{C} \min\left\{\frac{t^2}{4\|\bar{f}\|_{L^2}^2 \|\bar{K}_{SE}\|_{op}}, \frac{t}{2\|\bar{f}\|_{op}}\right\}\right),$$

where $\phi_{\bar{f}}(\bar{g}) = \int_{\bar{\Omega}} \int_{\bar{\Omega}} \bar{g}(x) \bar{f}(x, y) \bar{g}(y) dx dy$ and $C = \max\{64, 54^2 8^4 / \|\bar{K}_{SE}\|_{op}\}$. Let $H_m(f)$ be defined as in [\(3.1\)](#). Furthermore, note that $\|\bar{f}\|_{L^2}^2 = m\|f\|_{L^2}^2$, $\|\bar{f}\|_{op} = \|f\|_{op}$, and $\|\bar{K}_{SE}\|_{op} = \|K_{SE}\|_{op}$. Then, if we let $t' = t/m$, we can rewrite [\(4.2\)](#) as

$$\mathbb{P}(|H_m(f) - \mathbb{E}[H_m(f)]| \geq t') \leq 54 \exp\left(-\frac{1}{C} \min\left\{\frac{mt'^2}{4\|f\|_{L^2}^2 \|K_{SE}\|_{op}}, \frac{mt'}{2\|f\|_{op}}\right\}\right).$$

By choosing $t' = 2\|f\|_{L^2} \sqrt{C \log(54/\delta) \|K_{SE}\|_{op}/m}$ and setting $\tilde{C} = C \log(54/\delta) \|K_{SE}\|_{op}$, we have

$$\mathbb{P}\left(|H_m(f) - \mathbb{E}[H_m(f)]| \geq 2\|f\|_{L^2} \sqrt{\frac{\tilde{C}}{m}}\right) \leq 54 \exp\left(-\min\left\{\log(54/\delta), 2\frac{\|f\|_{L^2}}{\|f\|_{op}} \sqrt{m\tilde{C}}\right\}\right).$$

The result follows by noting that $\|f\|_{L^2}/\|f\|_{op} \leq 1$ and $m \geq \frac{\log(54/\delta)}{4C\|K\|_{op}}$. \square

We can combine the result in [Theorem 4.4](#) with our bound for $\mathbb{E}[H_m(f)]$ to obtain a probabilistic bound in terms of $\text{tr}(f)$. In particular, combining [Theorem 4.1](#), [Theorem 4.4](#), and the triangle inequality gives the following corollary.

COROLLARY 4.5. *Let $f : \Omega \times \Omega \rightarrow \mathbb{R}$ be a continuous function with $\Omega = [a, b]$ and $-\infty < a < b < \infty$, where f can be written as $f = f_1 - f_2$ for some continuous PSD functions $f_1, f_2 : \Omega \times \Omega \rightarrow \mathbb{R}$. Let*

$$\ell < \min\left\{\frac{d}{2\sqrt{2} \log(8\|f\|_{\infty}(b-a)/\varepsilon)}, \frac{5\varepsilon}{52\|f\|_{\infty}}\right\},$$

$$m \geq \log\left(\frac{54}{\delta}\right) \max\left\{\frac{16C\|K_{SE}\|_{op}}{\varepsilon^2}, \frac{1}{4C\|K_{SE}\|_{op}}\right\},$$

where $d = d(\varepsilon) > 0$ is such that $|f(x, y) - f(x, z)| \leq \frac{\varepsilon}{4(b-a)}$ for all $y, z \in \Omega$ such that $|y - z| < d$ and $C = \max\{64, 54^2 8^4 / \|K_{SE}\|_{op}\}$. Then with probability $\geq 1 - \delta$,

$$|H_m(f) - \text{tr}(f)| \leq \varepsilon \|f\|_{L^2}.$$

where $H_m(f)$ is the continuous Hutchinson's estimate of $\text{tr}(f)$ computed with m probe functions drawn from $\mathcal{GP}(0, K_{SE})$ where K_{SE} has length-scale parameter ℓ .

When f is symmetric PSD, we have that $\|f\|_{L^2}^2 = \sum_i \lambda_i^2 \leq \lambda_1 \sum_i \lambda_i = \lambda_1 \text{tr}(f) \leq \text{tr}(f)^2$, where λ_i is the i th eigenvalue of F . Thus, for symmetric PSD functions, the result above gives a relative accuracy for the continuous Hutchinson's estimate of the trace of f .

5. ContHutch++. For continuous, symmetric PSD functions f , we can improve the bound for Hutchinson's estimator by projecting off a low-rank approximation of F corresponding to its first few largest eigenvalues. To understand why, note that Hutchinson's estimator error bound for symmetric PSD functions is only tight when the first few eigenvalues of F are much larger than the rest so that $\text{tr}(f) \approx \|f\|_{L^2}$. Thus, if we project off the first few eigenvalues of F , we can use Hutchinson's estimator to estimate the trace of the resulting function with smaller eigenvalues. We use the continuous randomized range finder, presented in [3], to compute the approximate projection from the first few eigenfunctions.

In [Theorem 5.1](#), we bound the difference between a symmetric, PSD, continuous function and its rank k approximation (that is, $\sum_{j=k+1}^{\infty} \sigma_j^2$) in terms of $\text{tr}(f)$.

THEOREM 5.1. *Let F_k be the best rank k approximation to the integral operator F defined by a symmetric, PSD, continuous function f . Then,*

$$\|F - F_k\|_{HS} \leq \frac{1}{\sqrt{k}} \text{tr}(f).$$

Proof. Since f is symmetric PSD and continuous, its eigendecomposition exists and converges absolutely and uniformly by Mercer's Theorem. Let $\lambda_1 \geq \lambda_2 \geq \dots \geq 0$ be the eigenvalues of F . Thus, we have that

$$\lambda_{k+1} \leq \frac{1}{k} \sum_{i=1}^k \lambda_i \leq \frac{1}{k} \text{tr}(f).$$

We can use this result to bound the error in the best rank k approximation by

$$\|F - F_k\|_{HS}^2 = \sum_{i=k+1}^{\infty} \lambda_i^2 \leq \lambda_{k+1} \sum_{i=k+1}^{\infty} \lambda_i \leq \frac{1}{k} \text{tr}(f) \sum_{i=k+1}^{\infty} \lambda_i \leq \frac{1}{k} \text{tr}(f)^2. \quad \square$$

Given a decomposition of $\text{tr}(f)$ such that $\text{tr}(f) = \text{tr}(f_1) + \text{tr}(f_2)$ where the L^2 norm of f_2 is bounded with high probability, we show that the approximation of $\text{tr}(f)$ given by computing $\text{tr}(f_1)$ exactly and $\text{tr}(f_2)$ using the continuous Hutchinson's estimator gives an accurate trace estimate with high probability for sufficient choices of m and ℓ .

THEOREM 5.2. *Let $f : \Omega \times \Omega \rightarrow \mathbb{R}$ be continuous, symmetric, and PSD, $\varepsilon > 0$, $0 < \delta < 1$, and $m, k \in \mathbb{N}$. Let $f_1, f_2 : \Omega \times \Omega \rightarrow \mathbb{R}$ be functions that satisfy $\text{tr}(f) = \text{tr}(f_1) + \text{tr}(f_2)$ and $\|f_2\|_{L^2} \leq \eta \|F - F_k\|_{HS}$ with probability $1 - \delta/2$ for some η , which may depend on the kernel K_{SE} and the eigenvalues of F . Let $k = c\sqrt{\log(108/\delta)}/\varepsilon$ for some positive constant c such that $k \in \mathbb{N}$. Let $d = d(\varepsilon) > 0$ satisfy $|f(x, y) - f(x, z)| \leq \frac{\varepsilon}{4(b-a)}$ for all $y, z \in \Omega$ such that $|y - z| < d$. Then for $C = \max\{64, 54^2 8^4 / \|K\|_{op}\}$, if*

$$m \geq \sqrt{\log(108/\delta)} \max \left\{ \frac{16C\eta^2 \|K_{SE}\|_{op}}{c\varepsilon}, \frac{1}{4C\|K_{SE}\|_{op}} \right\},$$

$$\ell < \min \left\{ \frac{d(\varepsilon\sqrt{k}/\eta)}{2\sqrt{2\log(8\eta\|f\|_{\infty}(b-a)/(\varepsilon\sqrt{k}))}}, \frac{5\varepsilon\sqrt{k}}{52\eta\|f\|_{\infty}} \right\},$$

then $Z = \text{tr}(f_1) + H_m(f_2)$, where H_m is the Hutchinson's estimator with length-scale parameter ℓ , satisfies

$$\mathbb{P}(|Z - \text{tr}(f)| \geq \varepsilon \text{tr}(f)) \leq \delta.$$

Proof. We have

$$|Z - \text{tr}(f)| = |H_m(f_2) - \text{tr}(f_2)| \leq \frac{\varepsilon\sqrt{k}}{\eta} \|f\|_{L^2},$$

with probability $\geq 1 - \delta/2$, where the inequality comes from the continuous Hutchinson's bound in [Corollary 4.5](#), and where $C = \max\{64, 54^2 8^4 / \|K\|_{op}\}$. Then, by our assumption on f_2 , we have

$$|Z - \text{tr}(f)| \leq \varepsilon\sqrt{k} \|F - F_k\|_{HS},$$

with probability $\geq 1 - \delta$. Finally, by [Theorem 5.1](#), we can rewrite the bound in terms of $\text{tr}(f)$: □

$$\mathbb{P}(|Z - \text{tr}(f)| \leq \varepsilon \text{tr}(f)) \geq 1 - \delta.$$

We can now choose such a decomposition $F = F_1 + F_2$ and use the continuous randomized range finder to get an error bound on the ContHutch++ trace estimate of f , given by Z . Let Q be the $\Omega \times n$ quasimatrix found from the continuous randomized rangefinder applied to F . The range of Q approximates the range of F with high probability. In particular, [\[3, Theorem 1\]](#) says that if we use the continuous randomized range finder on F with target rank $k \geq 1$ and oversampling parameter $p \geq 4$ (choosing $n = k + p$), then for any $t \geq 1$, $s \geq 2$ we have that

$$(5.1) \quad \|F - QQ^T F\|_{HS} \leq \sqrt{1 + t^2 s^2 \frac{3}{\gamma_k} \frac{k(k+p)}{p+1} \sum_{j=1}^{\infty} \frac{\lambda_j}{\lambda_1} \left(\sum_{i=k+1}^{\infty} \sigma_i^2 \right)^2},$$

with probability $\geq 1 - t^{-p} - e^{-s^2}$, where $\lambda_1 \geq \lambda_2 \geq \dots \geq 0$ are the eigenvalues of K_{SE} and $\gamma_k = k/(\lambda_1 \text{tr}(\tilde{K}^{-1}))$ with $\tilde{K}_{ij} = V_i^* K V_j$, where V_k is the $\Omega \times k$ quasimatrix of the first k right singular vectors of F .

Using the continuous randomized range finder, we can write F as

$$F = (QQ^T(FQQ^T)) + (FQQ^T + QQ^T F - 2QQ^T(FQQ^T) + (I - QQ^T)(F(I - QQ^T))).$$

Since F is the integral operator with continuous, PSD, symmetric kernel f , $\text{tr}(F) = \text{tr}(f)$. If we take the trace of the first and the second terms above, we find that they are equal to $\text{tr}(QQ^T FQQ^T)$ and $\text{tr}((I - QQ^T)F(I - QQ^T))$, respectively. Thus, we choose

$$\begin{aligned} F_1 &= QQ^T FQQ^T, \\ F_2 &= (I - QQ^T)(F(I - QQ^T)). \end{aligned}$$

This choice ensures that the functions defining F_1 and F_2 are symmetric PSD. Furthermore, F_1 and F_2 are both trace class since their traces are bounded by $\text{tr}(f)$. Since traces are cyclic, we find that

$$\begin{aligned} \text{tr}(F_1) &= \text{tr}(Q^T FQ), \\ \text{tr}(F_2) &= \text{tr}((I - QQ^T)(F(I - QQ^T))). \end{aligned}$$

We directly compute the quantity $\text{tr}(F_1)$ since $Q^T FQ$ is an $n \times n$ matrix. We use Hutchinson's estimator to approximate $\text{tr}(F_2)$. The trace of F_1 requires n operator-function products, i.e.,

$$\text{tr}(F_1) = \sum_{i=1}^n \int_{\Omega} \int_{\Omega} q_i(x) f(x, y) q_i(y) dx dy,$$

We can use the continuous randomized range finder bound, given in [\(5.1\)](#), to bound the error on applying the continuous Hutchinson's estimator to F_2 . First, note that $\text{tr}(F_2) = \text{tr}((I - QQ^T)F)$ since the trace is cyclic and the projection $I - QQ^T$ has the property that $(I - QQ^T) = (I - QQ^T)^2$. Thus, computing the continuous Hutchinson's estimate of $\text{tr}(F_2)$ gives a bound in terms of $\|F - QQ^T F\|_{HS}$, which we can bound using the continuous randomized range finder. That is, if we choose $n = k + p$ functions drawn from the Gaussian process $\mathcal{GP}(0, K)$, we can apply [Theorem 5.2](#) to F_1 and F_2 , with

$$(5.2) \quad \eta = \sqrt{1 + t^2 s^2 \frac{3}{\gamma_k} \frac{k(k+p)}{p+1} \sum_{j=1}^{\infty} \frac{\lambda_j}{\lambda_1}}.$$

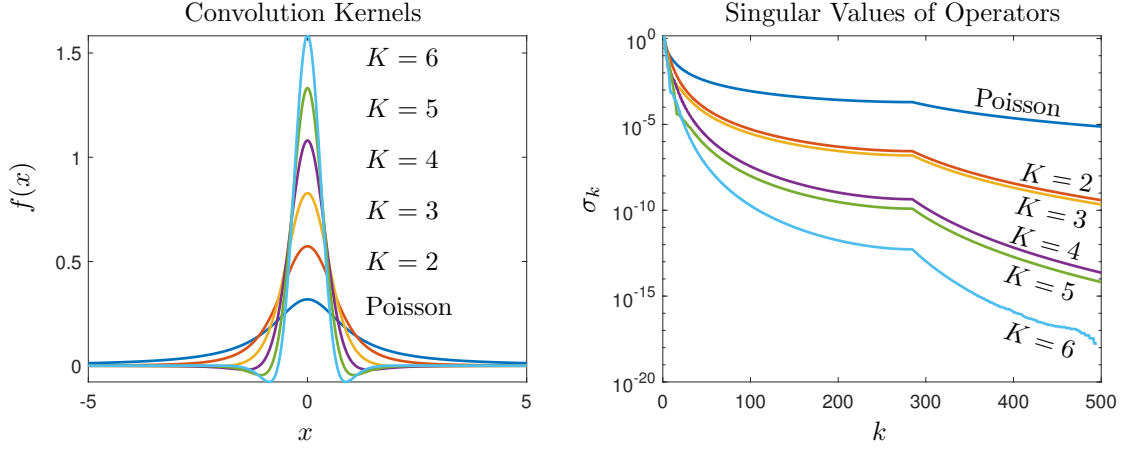


Fig. 6.1: The first six rational convolution kernels based on equispaced points are plotted in the left panel. The eigenvalues of the corresponding operators in (6.4) with $\mathcal{L} = -\Delta$, $\lambda = 10$, and $\sigma = 0.25$, are plotted in the right panel.

In particular, if we choose $k \geq 1/\varepsilon$, $p = \max\{5, \log_2(4/\delta)\}$, $t = 2$, and $s = \max\{2, \sqrt{\log_2(4/\delta)}\}$ in (5.1), then we can apply Theorem 5.2 to obtain the result in Corollary 5.3.

COROLLARY 5.3. *Let $f : \Omega \times \Omega \rightarrow \mathbb{R}$ be continuous, symmetric, and PSD, $\varepsilon > 0$, $0 < \delta < 1$, and $m, k \in \mathbb{N}$. Let $k = c\sqrt{\log(108/\delta)}/\varepsilon$ for some positive constant c such that $k \in \mathbb{N}$. Let Hutch++(f) be the continuous Hutch++ estimator of $\text{tr}(f)$ with covariance kernel K_{SE} with parameter ℓ , and oversampling parameter $p = \max\{5, \log_2(4/\delta)\}$, where m and ℓ satisfy*

$$m \geq \sqrt{\log(108/\delta)} \max \left\{ \frac{16C\eta^2 \|K\|_{op}}{c\varepsilon}, \frac{1}{4C\|K\|_{op}} \right\},$$

$$\ell < \min \left\{ \frac{d(\varepsilon\sqrt{k}/\eta)}{2\sqrt{2\log(8\eta\|f\|_\infty(b-a)/(\varepsilon\sqrt{k}))}}, \frac{5\varepsilon\sqrt{k}}{52\eta\|f\|_\infty} \right\}.$$

Then Hutch++(f) satisfies

$$(5.3) \quad |\text{Hutch++}(f) - \text{tr}(f)| \leq \varepsilon \text{tr}(f)$$

with probability $\geq 1 - \delta$, where $C = \max\{64, 54^2 8^4 / \|K\|_{op}\}$, $s = \max\{2, \sqrt{\log_2(4/\delta)}\}$, and

$$\eta = \sqrt{1 + 4s^2 \frac{3}{\gamma_k} \frac{k(k+p)}{p+1} \sum_{j=1}^{\infty} \frac{\lambda_j}{\lambda_1}}.$$

Here, $\lambda_1 \geq \lambda_2 \geq \dots \geq 0$ are the eigenvalues of K_{SE} and $\gamma_k = k/(\lambda_1 \text{tr}(\tilde{K}^{-1}))$ with $\tilde{K}_{ij} = V_i^* K V_j$, where V_k is the $\Omega \times k$ quasimatrix of the first k right singular vectors of F .

6. Numerical Experiments. We now apply ContHutch++ to two infinite-dimensional trace estimation problems that arise in physical applications. First, we combine ContHutch++ with rational smoothing kernels and demonstrate a new fast and accurate algorithm to compute the density-of-states (DOS) of Schrödinger operators. Second, we illustrate how ContHutch++ can efficiently and robustly calculate mean-field quantities that appear in photonic design problems with incoherent sources.

6.1. Example 1: Density-of-states for Schrödinger operators. A non-dimensionalized Schrödinger operator on a finite interval of length $2L$ takes the form

$$(6.1) \quad [\mathcal{L}u](x) = [-\Delta + v(x)]u(x), \quad x \in [-L, L],$$

where Δ is the Laplacian operator, $v(x)$ is a potential function, and $u(x)$ satisfies homogeneous Dirichlet or periodic boundary conditions on the boundary of the box. The eigenvalues of \mathcal{L} govern the observable

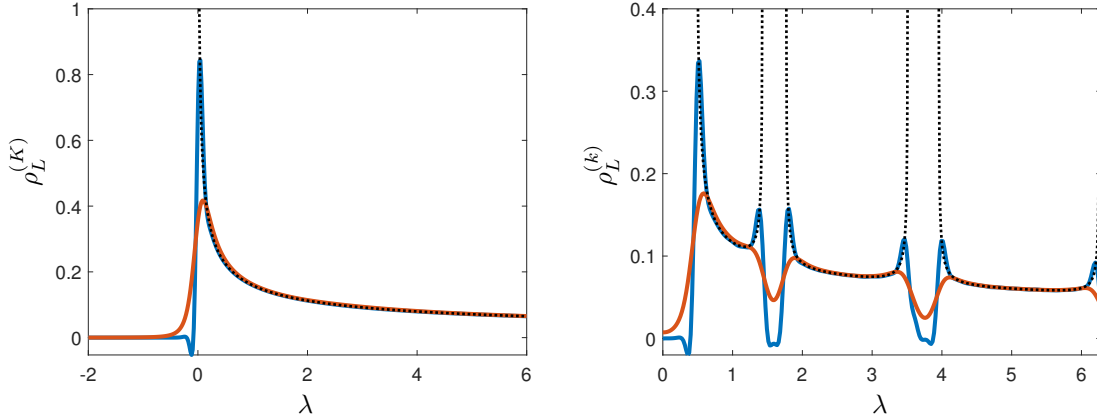


Fig. 6.2: Smoothed approximate density-of-states for the free particle (left) and the Kronig–Penney model (right) were computed using rational kernels of order $K = 2$ (red) and $K = 8$ (blue). The smoothed approximations are compared with analytic formulas (dotted lines) for the density-of-states in the asymptotic limit $L \rightarrow \infty$.

energy spectrum of a variety of quantum systems, and many important physical quantities can be calculated from their asymptotic density, which is known as the density-of-states and is defined as

$$(6.2) \quad \rho_L(\lambda) = \frac{1}{2L} \sum_{k=1}^{\infty} \delta(\lambda - \lambda_k).$$

Here, $\lambda_1, \lambda_2, \lambda_3, \dots$ are the eigenvalues of \mathcal{L} and $\delta(\cdot)$ is the Dirac delta measure with unit mass at the origin. The discrete measure $\rho_L(\lambda)$ often converges to an absolutely continuous measure with a piece-wise smooth density in the so-called “thermodynamic limit” $L \rightarrow \infty$.

The density-of-states can be approximated numerically by exploiting a link with the trace of the resolvent operator. After convolution with the Poisson kernel, a smoothed density-of-states is given by

$$(6.3) \quad \rho_L^\sigma(\lambda) = \frac{1}{2L} \sum_{k=1}^{\infty} \frac{\sigma}{(\lambda - \lambda_k)^2 + \sigma^2} = \frac{1}{2L} \text{tr} [\text{Im}(\mathcal{L} - \lambda - i\sigma)^{-1}].$$

As the smoothing parameter $\sigma \rightarrow 0$, $\rho_L^\sigma \rightarrow \rho_L$ weakly in the sense of measures. Numerically, σ and the discretization of the resolvent in (6.3) must be refined with caution to avoid instability caused by finite-size effects, as discussed in the closely related context of spectral measures of self-adjoint operators [6, 10]. Instead, we use ContHutch++ to compute the trace of the resolvent, balancing the trace estimation target accuracy with asymptotically tight smoothing error bounds for $\sigma > 0$ [6].

For two reasons, achieving high-accuracy density-of-states calculations with the Poisson kernel is challenging. First, ρ_L^σ converges slowly as $\sigma \rightarrow 0$, and smaller values of σ require larger discretizations of the resolvent. Second, the filtered resolvent operator in (6.3) has a slowly decaying spectrum because of the slow decay of the Poisson kernel. Consequently, many operator-function products are required for an accurate trace estimate. We can mitigate both challenges by smoothing $\rho_L(\lambda)$ with higher-order rational convolution kernels, introduced for high-resolution computation of spectral measures, instead of the Poisson kernel [6, 7]. A smoothed density-of-states obtained from a K th order rational kernel with simple poles p_1, \dots, p_K in the upper complex half-plane and residues r_1, \dots, r_K takes the form

$$(6.4) \quad \rho_L^{(K)}(\lambda) = \frac{1}{2L} \text{tr} \left[\text{Im} \sum_{j=1}^K r_j (\mathcal{L} - \lambda + p_j \sigma)^{-1} \right].$$

Six rational kernels with equispaced poles along $\text{Im}(z) = 1$ are plotted in Figure 6.1 (left) along with the eigenvalues associated with the trace estimation problems for the free particle (right), where $v(x) = 0$.

Figure 6.2 compares smoothed approximations to the density-of-states for a free particle (left) and the Kronig–Penney model (right) with analytic formulas for the exact thermodynamic limit (dotted

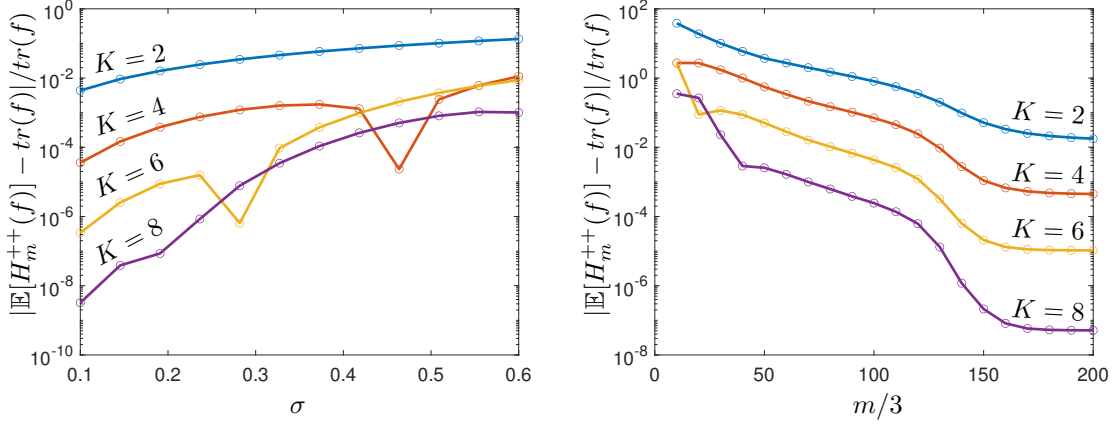


Fig. 6.3: Point-wise smoothing rates (left) and sample rates (right) of convergence of $\rho_{150}^{(K)}(1)$ for a free particle, with smoothing kernel orders $K = 2, 4, 6, 8$. Note that the relative errors in the right panel are plotted against $m/3$, the subspace dimension used for the randomized SVD and Hutchinson’s estimate. The number of function samples was fixed at $m = 600$ for the smoothing rate experiment (left), and the smoothing parameter was fixed at $\sigma = 0.2$ for the sample rate experiment (right).

line). The $K = 8$ smoothing kernel (red) gives much sharper results than the $K = 2$ kernel (blue) but takes negative values near endpoint singularities because the kernel is non-positive. A smoothing parameter of $\sigma = 0.2$ is employed for both experiments, and the resolvent was approximated on intervals with $L = 150$ and $L = 20\pi$ for the free particle and the Kronig–Penney model, respectively.

In Figure 6.3, the mean relative error in the density-of-states, evaluated at $\lambda = 1$, for the free particle is plotted against the smoothing parameter σ (left), and the number of operator-function products, m , used in ContHutch++ (right). Note that we plot the relative error against $m/3$, which is the dimension of the subspace used for the randomized SVD and Hutchinson’s estimate that are combined in the Hutch++ estimate. The domain size is $L = 150$, and the random function samples in ContHutch++ are drawn from a Gaussian process generated by the squared-exponential covariance kernel with parameter $\ell = 2L \times 10^{-3}$. The resolvent action is computed with a maximum discretization size of $N = 4100$. The order of convergence in the smoothing parameter increases with the order of the smoothing kernel. The accuracy also improves with the number of function samples until saturating at a limiting accuracy due to smoothing. With a fixed number of samples, the higher-order kernels are more accurate due to the faster spectral decay of the filtered operator (see Figure 6.1).

6.2. Example 2: Mean field intensity from incoherent sources. A recent body of work in photonic design [23, 22, 30] formulates essential physical quantities, such as average field intensity and power emission, as the trace of a self-adjoint, semi-definite operator related to the solution of Maxwell’s equations. Efficient optimization schemes leverage low-rank structure in the operator to optimize the trace without explicitly forming discretizations of the operator, which is prohibitively expensive. Interestingly, the spectral profile of this operator can depend on the material parameters, geometry, and separation between the current sources and the target emission region, some or all of which may vary during optimization. This section illustrates how ContHutch++ can robustly calculate the mean-square field intensity in a dielectric tube induced by spatially uncorrelated currents.

Consider a z -invariant dielectric tube whose cross-section $\Omega \subset \mathbb{R}^2$ has a Hölder continuous boundary. According to Maxwell’s equations, a time-harmonic current with frequency ω and amplitude $b(x, y)$ in the z -direction produces an electric field E_z in the z -direction satisfying (after nondimensionalization)

$$(6.5) \quad \Delta E_z - \omega^2 \epsilon(x, y) E_z = i\omega b(x, y), \quad \text{where} \quad (x, y) \in \mathbb{R}^2.$$

Here, $\epsilon(x, y)$ is the dielectric function, smoothly interpolating between the background’s relative permittivity of $\epsilon_1 = 1$ and the dielectric’s relative permittivity of $\epsilon_2 = 12$, so that

$$(6.6) \quad \epsilon(x, y) = \epsilon_1 + \xi_\sigma(x, y)(\epsilon_2 - \epsilon_1), \quad \text{where} \quad \xi_\sigma(x, y) = \frac{1}{(\sigma\sqrt{2\pi})^2} \int_{\Omega} e^{-\frac{(y-y')^2 + (x-x')^2}{2\sigma^2}} dx' dy'.$$

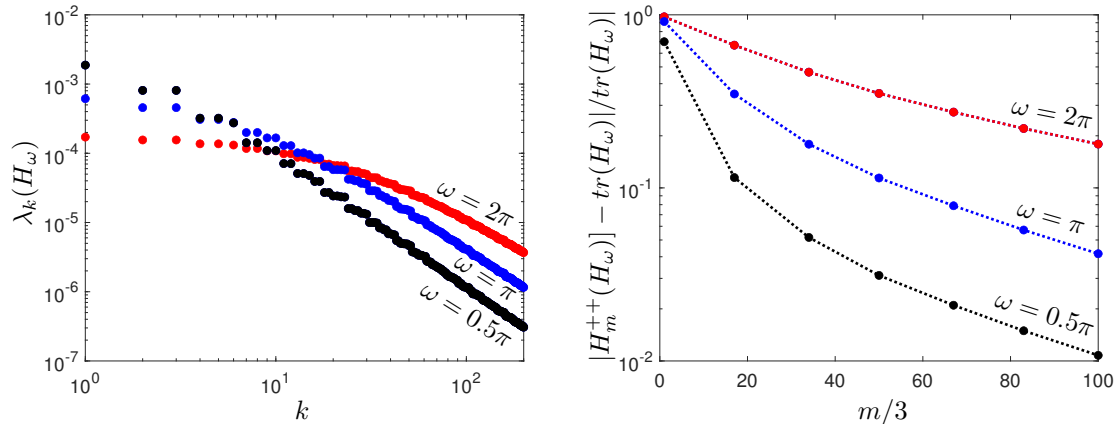


Fig. 6.4: Plotted in the left panel are the first 200 eigenvalues of the operator in (6.7), whose trace corresponds to the mean field intensity due to spatially incoherent current sources with frequency ω in a dielectric tube with circular cross-section of radius $r = 0.5$. As the angular frequency ω increases from $\pi/2$ to 2π , the leading spectrum of the operator becomes increasingly flat and takes longer to approach the asymptotic algebraic decay rate. In the right panel, we plot the relative error in the Hutch++ trace estimate as the number of source samples increases from $m = 3, \dots, 300$.

The interpolation parameter $\sigma > 0$ controls the sharpness of the transition between the dielectric and background materials. In the limit of spatially uncorrelated currents, used to model fields in fluorescent materials and other processes of spontaneous emission, the mean-square field intensity is given by [30]

$$(6.7) \quad \langle E_z \rangle = \mathbb{E} \left[\frac{1}{|\Omega|} \int_{\Omega} |E_z(x, y)|^2 dx dy \right] = \frac{1}{|\Omega|} \text{tr} [(A_\omega M_\Omega)^\dagger M_\Omega (A_\omega M_\Omega)].$$

Here, A_ω represents the solution operator mapping the current source b in the dielectric to the field E_z in (6.5). M_Ω represents multiplication by the smoothed characteristic function ξ_σ in (6.6). Note that the spectrum of the self-adjoint operator $H_\omega = (A_\omega M_\Omega)^\dagger M_\Omega (A_\omega M_\Omega)$ typically decays slowly because the target field and the current source are both supported in the dielectric cross-section, Ω . Figure 6.4 (left panel) displays the first 200 eigenvalues of H_ω for a circular cross-section $\Omega = \{(x, y) \in \mathbb{R}^2 : x^2 + y^2 \leq (0.5)^2\}$ with angular frequency values $\omega = 0.5\pi, \pi$, and 2π .

To approximate operator-function products with H_ω , we discretize (6.5) with second-order centered finite differences on the unit square $[-1, 1]^2 \subset \mathbb{R}^2$, surrounded by a perfectly matched layer (PML) with unit thickness and strength, and prescribe homogeneous Dirichlet boundary conditions on the outer edges of the PML [20]. The dielectric cross-section Ω is scaled so that its diameter is inscribed in a disk of radius $r = 0.5$ centered at the origin. Each numerical experiment in this section uses 100 grid points in each direction on the unit square, and the interpolation parameter $\sigma > 0$ in (6.6) is half the distance between grid points. The Gaussian process used for randomized trace estimation is formed from the tensor product of squared exponential kernels on the unit square with length-scale parameter $\ell = 0.08$. The refinement of the Hutch++ estimator with increasing sample size, m , is verified numerically for the circular cross-section in the right panel of Figure 6.4 with $\omega = 0.5\pi, \pi$, and 2π . Figure 6.5 displays a few random source currents, $b(x, y)$, used for trace estimation, the resulting field intensities, $|E_z(x, y)|^2$, and the estimated average field intensity $\langle E_z \rangle$ from (6.7) for three dielectric cross-sections: a disk (left panel), a quadrifolium (middle panel), and a disk with an astroid cutout (right panel). The respective trace estimates computed by ContHutch++ are $\langle E_z \rangle \approx 0.0069$ (disk), 0.0071 (quadrifolium), and 0.0069 (disk with astroid cutout).

REFERENCES

- [1] R. ADAMCZAK, *A note on the Hanson-Wright inequality for random vectors with dependencies*, Electronic Communications in Probability, 20 (2015), pp. 1–13.
- [2] H. AVRON AND S. TOLEDO, *Randomized algorithms for estimating the trace of an implicit symmetric positive semi-definite matrix*, Journal of the ACM (JACM), 58 (2011), pp. 1–34.

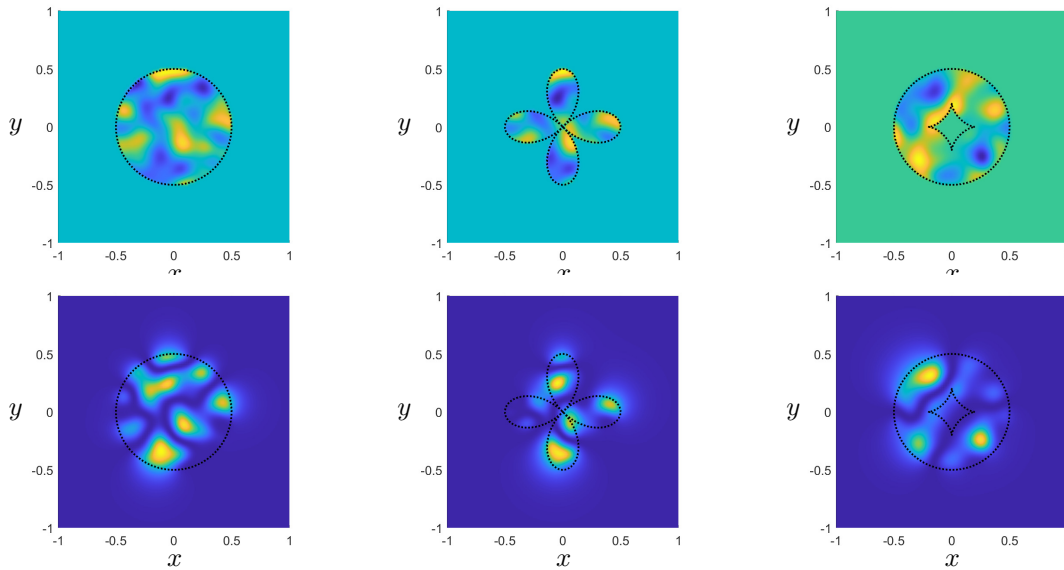


Fig. 6.5: Sample current sources $b(x, y)$ (top) and field intensities $|E_z(x, y)|^2$ (bottom), with frequency $\omega = \pi$, for the circle (left), quadrifolium (middle), and circle with an astroid cutout (right) cross-sections of diameter 0.5. The trace estimates computed by ContHutch++ are $\langle E_z \rangle \approx 0.0069$ (left), 0.0071 (middle), and 0.0069 (right). The boundary of Ω is marked with a dashed line in each panel.

- [3] N. BOULLÉ AND A. TOWNSEND, *Learning elliptic partial differential equations with randomized linear algebra*, Found. Comput. Math., (2022), pp. 1–31.
- [4] C. BRISLAWN, *Kernels of trace class operators*, Proc. Am. Math. Soc., 104 (1988), pp. 1181–1190.
- [5] T. CHEN AND E. HALLMAN, *Krylov-aware stochastic trace estimation*, SIAM J. Matrix Anal. Appl., 44 (2023), pp. 1218–1244.
- [6] M. COLBROOK, A. HORNING, AND A. TOWNSEND, *Computing spectral measures of self-adjoint operators*, SIAM Rev., 63 (2021), pp. 489–524.
- [7] M. J. COLBROOK, A. HORNING, K. THICKE, AND A. B. WATSON, *Computing spectral properties of topological insulators without artificial truncation or supercell approximation*, IMA J. Appl. Math., 88 (2023), pp. 1–42.
- [8] A. CORTINOVIS AND D. KRESSNER, *On randomized trace estimates for indefinite matrices with an application to determinants*, Found. Comput. Math., (2021), pp. 1–29.
- [9] C. DE BOOR, *An alternative approach to (the teaching of) rank, basis, and dimension*, Lin. Alg. Appl., 146 (1991), pp. 221–229.
- [10] M.-S. DUPUY AND A. LEVITT, *Finite-size effects in response functions of molecular systems*, SMAI J. Comput. Math., (2022).
- [11] E. EPPERLY, *Note to self: Hanson–Wright inequality*, 2022.
- [12] E. N. EPPERLY, J. A. TROPP, AND R. J. WEBBER, *XTrace: Making the most of every sample in stochastic trace estimation*, (2023).
- [13] A. FROMMER, M. N. KHALIL, AND G. RAMIREZ-HIDALGO, *A multilevel approach to variance reduction in the stochastic estimation of the trace of a matrix*, SIAM J. Sci. Comput., 44 (2022), pp. A2536–A2556.
- [14] N. HALKO, P.-G. MARTINSSON, AND J. A. TROPP, *Finding structure with randomness: Probabilistic algorithms for constructing approximate matrix decompositions*, SIAM Rev., 53 (2011), pp. 217–288.
- [15] E. HALLMAN AND D. TROESTER, *A multilevel approach to stochastic trace estimation*, Linear Algebra Appl., 638 (2022), pp. 125–149.
- [16] M. F. HUTCHINSON, *A stochastic estimator of the trace of the influence matrix for Laplacian smoothing splines*, Communications in Statistics-Simulation and Computation, 18 (1989), pp. 1059–1076.
- [17] L. LIN, *Randomized estimation of spectral densities of large matrices made accurate*, Numer. Math., 136 (2017), pp. 183–213.
- [18] L. LIN, Y. SAAD, AND C. YANG, *Approximating spectral densities of large matrices*, SIAM Rev., 58 (2016), pp. 34–65.
- [19] R. A. MEYER, C. MUSCO, C. MUSCO, AND D. P. WOODRUFF, *Hutch++: Optimal stochastic trace estimation*, in Symposium on Simplicity in Algorithms (SOSA), SIAM, 2021, pp. 142–155.
- [20] A. OSKOOI AND S. G. JOHNSON, *Distinguishing correct from incorrect PML proposals and a corrected unsplit PML for anisotropic, dispersive media*, J. Comput. Phys., 230 (2011), pp. 2369–2377.
- [21] D. PERSSON, A. CORTINOVIS, AND D. KRESSNER, *Improved variants of the Hutch++ algorithm for trace estimation*, SIAM J. Matrix Anal. Appl., 43 (2022), pp. 1162–1185.
- [22] A. G. POLIMERIDIS, M. T. H. REID, W. JIN, S. G. JOHNSON, J. K. WHITE, AND A. W. RODRIGUEZ, *Fluctuating volume-current formulation of electromagnetic fluctuations in inhomogeneous media: Incandescence and luminescence in arbitrary geometries*, Phys. Rev. B, 92 (2015), p. 134202.

- [23] A. W. RODRIGUEZ, O. ILIC, P. BERMEL, I. CELANOVIC, J. D. JOANNOPOULOS, M. SOLJAČIĆ, AND S. G. JOHNSON, *Frequency-selective near-field radiative heat transfer between photonic crystal slabs: A computational approach for arbitrary geometries and materials*, Phys. Rev. Lett., 107 (2011), p. 114302.
- [24] F. SMITHIES, *The Eigen-Values and Singular Values of Integral Equations†*, Proceedings of the London Mathematical Society, s2-43 (1938), pp. 255–279.
- [25] G. W. STEWART, *Matrix Algorithms: Volume 1: Basic Decompositions*, SIAM, 1998.
- [26] A. TOWNSEND AND L. N. TREFETHEN, *Continuous analogues of matrix factorizations*, P. Roy. Soc. A, 471 (2015), p. 20140585.
- [27] L. N. TREFETHEN AND D. BAU III, *Numerical linear algebra*, SIAM, 1997.
- [28] S. UBARU, J. CHEN, AND Y. SAAD, *Fast estimation of $\text{tr}(f(a))$ via stochastic Lanczos quadrature*, SIAM J. Matrix Anal. Appl., 38 (2017), pp. 1075–1099.
- [29] A. WEISSE, G. WELLEIN, A. ALVERMANN, AND H. FEHSKE, *The kernel polynomial method*, Rev. Mod. Phys., 78 (2006), p. 275.
- [30] W. YAO, F. VERDUGO, R. E. CHRISTIANSEN, AND S. G. JOHNSON, *Trace formulation for photonic inverse design with incoherent sources*, Struct. Multidiscipl. Optim., 65 (2022), p. 336.

Appendix A. A Continuous Hanson–Wright Inequality. We first need the following definition and two lemmas to prove the Continuous Hanson-Wright Inequality. First, we must establish the idea of the convex concentration property for functions. The following definition is a continuous analogue of [1, Definition 2.2].

DEFINITION A.1. *Let g be a function drawn from a GP. We say that g has the convex concentration property with constant α if for every 1-Lipschitz convex operator $\phi : L^2(\Omega) \rightarrow \mathbb{R}$, we have $\mathbb{E}[|\phi(g)|] < \infty$ and*

$$(A.1) \quad \mathbb{P}(|\phi(g) - \mathbb{E}[\phi(g)]| \geq t) < 2 \exp(-t^2/\alpha^2), \quad t > 0.$$

Note that if $g \sim \mathcal{GP}(0, K_{SE})$, then g satisfies the convex concentration property with constant $\sqrt{2}$.

LEMMA A.2. *Let $K, V : \Omega \times \Omega \rightarrow \mathbb{R}$ be symmetric, PSD, and continuous functions, where $\Omega = [a, b]$ for $-\infty < a < b < \infty$. Then*

$$(A.2) \quad \text{tr}(W) \leq \text{tr}(V) \|K\|_{op},$$

where $W(s, t) = \int_{\Omega} K(s, z)V(z, t)dz$ and $\|K\|_{op}$ is the magnitude of the largest eigenvalue of K .

Proof. The trace of W is given by $\text{tr}(W) = \int_{\Omega} \int_{\Omega} K(s, z)V(z, s)dzds$. Since K is a continuous, symmetric positive semidefinite kernel, Mercer’s theorem tells us that there exists an orthonormal basis $\{u_i\}$ of $L^2(\Omega)$ such that the eigendecomposition of K , given by $K(s, z) = \sum_i \lambda_i u_i(s)u_i(z)$, converges absolutely and uniformly. Thus, substituting the eigendecomposition of K into the expression for $\text{tr}(W)$ gives

$$\text{tr}(W) = \sum_{i \in \mathbb{N}} \lambda_i \int_{\Omega} u_i(z) \int_{\Omega} V(z, s)u_i(s)dsdz.$$

However, for each $i \in \mathbb{N}$, $\lambda_i \leq \lambda_{\max} = \|K\|_{op}$, where the last equality comes from the fact that the eigenvalues of a positive semidefinite function are all non-negative. Thus,

$$(A.3) \quad \text{tr}(W) \leq \|K\|_{op} \sum_{i \in \mathbb{N}} \int_{\Omega} u_i(z) \int_{\Omega} V(z, s)u_i(s)dsdz.$$

Now we only need to show that $\sum_i \int_{\Omega} u_i(z) \int_{\Omega} V(z, s)u_i(s)dsdz = \text{tr}(V)$. Mercer’s theorem also tells us that there exists an eigendecomposition of V , given by $V(z, s) = \sum_j \mu_j v_j(z)v_j(s)$, where the functions v_j also form an orthogonal basis for $L^2(\Omega)$ and the sum converges absolutely and uniformly. Since the eigenfunctions of K form an orthonormal basis for $L^2(\Omega)$, there exists weights a_{ij} such that

$v_j(s) = \sum_i a_{ij} u_i(s)$ and $\sum_i a_{ij}^2 = 1$. Thus, we can rewrite (A.3) as

$$\begin{aligned}
\text{tr}(W) &\leq \|K\|_{op} \sum_{i \in \mathbb{N}} \int_{\Omega} u_i(z) \int_{\Omega} \sum_{j \in \mathbb{N}} \mu_j v_j(z) v_j(s) u_i(s) ds dz \\
&= \|K\|_{op} \sum_{i \in \mathbb{N}} \sum_{j \in \mathbb{N}} \mu_j \int_{\Omega} u_i(z) \int_{\Omega} \left(\sum_{k \in \mathbb{N}} a_{kj} u_k(z) \right) \left(\sum_{l \in \mathbb{N}} a_{lj} u_l(s) \right) u_i(s) ds dz \\
&= \|K\|_{op} \sum_{i \in \mathbb{N}} \sum_{j \in \mathbb{N}} \mu_j \int_{\Omega} u_i(z) \left(\sum_{k \in \mathbb{N}} a_{kj} u_k(z) \right) dz \int_{\Omega} u_i(s) \left(\sum_{l \in \mathbb{N}} a_{lj} u_l(s) \right) ds \\
&= \|K\|_{op} \sum_{j \in \mathbb{N}} \mu_j \sum_{i \in \mathbb{N}} a_{ij}^2 = \|K\|_{op} \text{tr}(V),
\end{aligned}$$

where $\int_{\Omega} u_i(z) \left(\sum_k a_{kj} u_k(z) \right) dz = \int_{\Omega} u_i(s) \left(\sum_{l \in \mathbb{N}} a_{lj} u_l(s) \right) ds = a_{ij}$ by orthogonality of the functions u_i . \square

LEMMA A.3. $h(g) = \|\phi'(g)\|_{L^2(\Omega)} = \left\| 2 \int_{\Omega} f(x, y) g(y) dy \right\|_{L^2(\Omega)}$ is $2\|f\|_{op}$ -Lipschitz. That is,

$$|h(g_1) - h(g_2)| \leq 2\|f\|_{op} \|g_1 - g_2\|_{L^2(\Omega)}.$$

Proof. We can prove this statement by rewriting an $L^2(\Omega)$ norm as an $L^2(\Omega \times \Omega)$ norm. The reverse triangle inequality tells us that

$$\begin{aligned}
\left| \|\phi'(g_1)\|_{L^2(\Omega)} - \|\phi'(g_2)\|_{L^2(\Omega)} \right| &\leq \|\phi'(g_1) - \phi'(g_2)\|_{L^2(\Omega)} \\
&= 2 \left\| \int_{\Omega} f(x, y) (g_1(x) - g_2(x)) dx \right\|_{L^2(\Omega)} \\
&= 2 \left(\int_{\Omega} \left(\int_{\Omega} f(x, y) (g_1(x) - g_2(x)) dx \right)^2 dy \right)^{1/2} \\
&\leq 2 \left(\int_{\Omega} \int_{\Omega} f(x, y)^2 (g_1(x) - g_2(x))^2 dx dy \right)^{1/2} \\
&= 2 \|f(x, y) (g_1(x) - g_2(x))\|_{L^2(\Omega \times \Omega)} \\
&\leq 2\|f\|_{op} \|g_1 - g_2\|_{L^2(\Omega)},
\end{aligned}$$

where $\|f\|_{op}$ equals the largest singular value of f . \square

A.1. Proof of the Continuous Hanson-Wright Inequality, Theorem 4.2.

Proof. Any discretization of the double integral in the definition of ϕ gives a product of the form $v^T A v$, where v is the discretization of g and A is the discretization of f . Since f is PSD, so is A . Thus, $v^T A v$ is convex with respect to v . Since this holds for any discretization, $\phi(g)$ is also convex. Taking the Fréchet derivative of ϕ with respect to g gives $\phi'(g) = 2 \int_{\Omega} f(x, y) g(y) dy$. Let $h = \|\phi'(g)\|_{L^2}$. Then, the expectation of h^2 is

$$\begin{aligned}
\mathbb{E}[h^2] &= \mathbb{E} \left[\left\| 2 \int_{\Omega} f(x, y) g(y) dy \right\|_{L^2}^2 \right] \\
&= 4 \mathbb{E} \left[\int_{\Omega} \left(\int_{\Omega} f(x, y) g(y) dy \right)^2 dx \right] \\
&= 4 \mathbb{E} \left[\int_{\Omega} \int_{\Omega} f(x, y) g(y) dy \int_{\Omega} f(x, z) g(z) dz dx \right] \\
&= 4 \int_{\Omega} \int_{\Omega} \int_{\Omega} f(x, z) f(x, y) \mathbb{E}[g(z) g(y)] dx dy dz \\
&= 4 \int_{\Omega} \int_{\Omega} K_{SE}(y, z) \int_{\Omega} f(x, z) f(x, y) dx dz dy.
\end{aligned}$$

However, since f is symmetric,

$$\int_{\Omega} \int_{\Omega} K_{SE}(y, z) \int_{\Omega} f(x, z) f(x, y) dx dz dy = \int_{\Omega} \int_{\Omega} K_{SE}(y, z) \int_{\Omega} f(z, x) f(x, y) dx dz dy.$$

Let $W(s, t) = \int_{\Omega} K(s, z) \int_{\Omega} f(z, x) f(x, t) dx dz$. Then $\mathbb{E}[h^2] = \text{tr}(W)$. Thus, by [Lemma A.2](#) with $V(z, t) = \int_{\Omega} f(z, x) f(x, t) dx$ and the fact that $\text{tr}(V) = \int_{\Omega} \int_{\Omega} f(z, x) f(x, z) dx dz = \|f\|_{L^2}^2$ we have

$$\mathbb{E}[h^2] \leq 4\|f\|_{L^2}^2 \|K_{SE}\|_{op}.$$

Thus, by Jensen's inequality,

$$(A.4) \quad \mathbb{E}[h] \leq 2\|f\|_{L^2} \|K_{SE}\|_{op}^{1/2}.$$

Let $B = \{g \in L^2(\Omega) : h(g) \leq 2\|f\|_{L^2} \|K_{SE}\|_{op}^{1/2} + \sqrt{t}\|f\|_{op}^{1/2}\}$. Then, since h is $2\|f\|_{op}$ -Lipschitz by [Lemma A.3](#), we can apply the convex concentration property to $h/(2\|f\|_{op})$ to get

$$\mathbb{P}(|h(g) - \mathbb{E}[h(g)]| \geq 2t\|f\|_{op}) \leq 2\exp(-t^2/2).$$

Using the change of variables $s = 2t\|f\|_{op}$, we find

$$\mathbb{P}(|h(g) - \mathbb{E}[h(g)]| \geq s) \leq 2\exp\left(\frac{-s^2}{8\|f\|_{op}^2}\right).$$

However, notice that we can use [\(A.4\)](#) to show that B contains the set $\{g \in L^2(\Omega) : h(g) - \mathbb{E}[h] \leq \sqrt{t}\|f\|_{op}^{1/2}\}$. Thus, $B^C \subseteq \{g \in L^2(\Omega) : |h(g) - \mathbb{E}[h]| \geq \sqrt{t}\|f\|_{op}^{1/2}\}$. Therefore,

$$\begin{aligned} \mathbb{P}(g \notin B) &\leq \mathbb{P}(|h(g) - \mathbb{E}[h(g)]| \geq \sqrt{t}\|f\|_{op}^{1/2}) \\ &\leq 2\exp\left(-\frac{t}{8\|f\|_{op}^2}\right). \end{aligned}$$

Define a new convex function $\tilde{\phi} : L^2(\Omega) \rightarrow \mathbb{R}$ by $\tilde{\phi}(\tilde{g}) = \max_{g \in B} \{\langle \phi'(g), \tilde{g} - g \rangle_{L^2} + \phi(g)\}$. We want to show that $\tilde{\phi}$ is also Lipschitz continuous so that we may use the convex concentration property. To do so, let $g_1, g_2 \in L^2(\Omega)$ and consider

$$\begin{aligned} \left| \tilde{\phi}(g_1) - \tilde{\phi}(g_2) \right| &= \left| \max_{g \in B} \{\langle \phi'(g), g_1 - g \rangle_{L^2} + \phi(g)\} - \max_{g \in B} \{\langle \phi'(g), g_2 - g \rangle_{L^2} + \phi(g)\} \right| \\ &\leq \left| \max_{g \in B} \{\langle \phi'(g), g_1 - g_2 \rangle_{L^2}\} \right| \\ &\leq \max_{g \in B} \int_{\Omega} |\phi'(g)(x)(g_1 - g_2)(x)| dx. \end{aligned}$$

Applying Hölder's inequality gives

$$\left| \tilde{\phi}(g_1) - \tilde{\phi}(g_2) \right| \leq \|g_1 - g_2\|_{L^2} \max_{g \in B} \|\phi'(g)\|_{L^2} = \|g_1 - g_2\|_{L^2} \max_{g \in B} h(g).$$

Since the maximum is taken over $g \in B$, we know that $h(g) \leq 2\|f\|_{L^2} \|K_{SE}\|_{op}^{1/2} + \sqrt{t}\|f\|_{op}^{1/2}$. Thus, we have

$$\left| \tilde{\phi}(g_1) - \tilde{\phi}(g_2) \right| \leq M\|g_1 - g_2\|_{L^2},$$

where $M = 2\|f\|_{L^2} \|K_{SE}\|_{op}^{1/2} + \sqrt{t}\|f\|_{op}^{1/2}$. Thus, $\tilde{\phi}$ is M -Lipschitz.

Then the convex concentration property gives

$$\mathbb{P}(|\tilde{\phi}(g) - \mathbb{E}[\tilde{\phi}(g)]| \geq s) \leq 2\exp\left(-\frac{s^2}{2M^2}\right).$$

Further, since ϕ is convex, $\phi(g_1) \geq \phi(g) + \langle \phi'(g), g_1 - g \rangle_{L^2}$ for all $g \in L^2(\Omega)$. Thus, $\phi(g_1) \geq \max_{g \in B} \{\phi(g) + \langle \phi'(g), g_1 - g \rangle_{L^2}\} = \tilde{\phi}(g_1)$. If we require that $g_1 \in B$ then we also have $\tilde{\phi}(g_1) = \max_{g \in B} \{\langle \phi'(g), g_1 - g \rangle_{L^2} + \phi(g)\} \geq \langle \phi'(g_1), g_1 - g_1 \rangle_{L^2} + \phi(g_1) = \phi(g_1)$. Thus, for $g_1 \in B$, $\tilde{\phi}(g_1) = \phi(g_1)$.

We can then use [1, Lemma 3.1] with $S = \tilde{\phi}(g)$, $Z = \phi(g)$, $a = 2\sqrt{2}\|f\|_{L^2}\|K_{SE}\|_{op}^{1/2}$, and $b = 8\|f\|_{op}$. Keeping track of constants in this lemma's proof gives us the result

$$\mathbb{P}(|\phi(g) - \text{Med}(\phi(g))| \geq t) \leq 27 \exp\left(-\frac{1}{32} \min\left\{\frac{t^2}{\|f\|_{L^2}^2 \|K_{SE}\|_{op}}, \frac{t}{\|f\|_{op}}\right\}\right),$$

where $\text{Med}(\phi(g))$ refers to the median of $\phi(g)$. However, we want a result in terms of the expected value of $\phi(g)$, not its median. To accomplish this, we use [1, Lemma 3.2], again keeping track of constants in the proof to get

$$\mathbb{P}(|\phi(g) - \mathbb{E}[\phi(g)]| \geq t) \leq 27 \exp\left(-\frac{1}{C} \min\left\{\frac{t^2}{\|f\|_{L^2}^2 \|K_{SE}\|_{op}}, \frac{t}{\|f\|_{op}}\right\}\right),$$

where $C = \max\{64, 54^2 8^4 / \|K_{SE}\|_{op}\}$. □

A.2. Proof of Continuous Hanson-Wright Inequality Corollary, Corollary 4.3.

Proof. Notice that even when f is not symmetric, we have

$$\int_{\Omega} \int_{\Omega} g(x) f(x, y) g(y) dx dy = \int_{\Omega} \int_{\Omega} g(x) f(y, x) g(y) dx dy.$$

Thus, the symmetric function $\tilde{f}(x, y) = \frac{1}{2}(f(x, y) + f(y, x))$ satisfies

$$\int_{\Omega} \int_{\Omega} g(x) \tilde{f}(x, y) g(y) dx dy = \int_{\Omega} \int_{\Omega} g(x) f(x, y) g(y) dx dy.$$

Further, $\|\tilde{f}\| \leq \frac{1}{2}(\|f\| + \|f^T\|) = \|f\|$, for both the L^2 norm and the operator norm. Thus, [Theorem 4.2](#) holds for both f_1 and f_2 . However, we want to find a bound for $f = f_1 - f_2$. Note that since $f = f_1 - f_2$, $\tilde{f} = \tilde{f}_1 - \tilde{f}_2$ where $\tilde{f}_1(x, y) = \frac{1}{2}(f_1(x, y) + f_1(y, x))$ and $\tilde{f}_2 = \frac{1}{2}(f_2(x, y) + f_2(y, x))$, so we can express everything in terms of \tilde{f}_1 and \tilde{f}_2 . For convenience, let ϕ_1 be defined in terms of \tilde{f}_1 , ϕ_2 be defined in terms of \tilde{f}_2 , and ϕ be defined in terms of f . Thus, we can simplify the probability in terms of f as

$$\begin{aligned} \mathbb{P}(|\phi(g) - \mathbb{E}[\phi(g)]| \geq t) &= \mathbb{P}(|\phi_1(g) - \phi_2(g) - \mathbb{E}[\phi_1(g) - \phi_2(g)]| \geq t) \\ &\leq \mathbb{P}(|\phi_1(g) - \mathbb{E}[\phi_1(g)]| + |\phi_2(g) - \mathbb{E}[\phi_2(g)]| \geq t) \\ &\leq \mathbb{P}(|\phi_1(g) - \mathbb{E}[\phi_1(g)]| \geq t/2) + \mathbb{P}(|\phi_2(g) - \mathbb{E}[\phi_2(g)]| \geq t/2), \end{aligned}$$

where the last line comes from the fact that to have $|\phi_1(g) - \mathbb{E}[\phi_1(g)]| + |\phi_2(g) - \mathbb{E}[\phi_2(g)]| \geq t$, we certainly need at least one of $|\phi_1(g) - \mathbb{E}[\phi_1(g)]|$ and $|\phi_2(g) - \mathbb{E}[\phi_2(g)]|$ to be at least $t/2$.

Let λ_i be the i th eigenvalue of \tilde{f} . Let $S = \{\lambda_i : \lambda_i \geq 0\}$. Note that $\|\tilde{f}_j\|_{op} \leq |\lambda_1| = \|\tilde{f}\|_{op}$ for $j = 1, 2$. Furthermore, $\|\tilde{f}_1\|_{L^2}^2 = \sum_{i \in S} \lambda_i^2 \leq \sum_{i=1}^{\infty} \lambda_i^2 = \|\tilde{f}\|_{L^2}^2$ and $\|\tilde{f}_2\|_{L^2}^2 = \sum_{i \in \mathbb{N}-S} \lambda_i^2 \leq \sum_{i=1}^{\infty} \lambda_i^2 = \|\tilde{f}\|_{L^2}^2$. Thus, we can write the probability bound in terms of the norm of f . That is, from [Theorem 4.2](#),

$$\begin{aligned} \mathbb{P}(|\phi(g) - \mathbb{E}[\phi(g)]| \geq t) &\leq 27 \exp\left(-\frac{1}{C} \min\left\{\frac{t^2}{4\|f_1\|_{L^2}^2 \|K_{SE}\|_{op}}, \frac{t}{2\|f_1\|_{op}}\right\}\right) \\ &\quad + 27 \exp\left(-\frac{1}{C} \min\left\{\frac{t^2}{4\|f_2\|_{L^2}^2 \|K_{SE}\|_{op}}, \frac{t}{2\|f_2\|_{op}}\right\}\right) \\ &\leq 54 \exp\left(-\frac{1}{C} \min\left\{\frac{t^2}{4\|f\|_{L^2}^2 \|K_{SE}\|_{op}}, \frac{t}{2\|f\|_{op}}\right\}\right), \end{aligned}$$

where $C = \max\{64, 54^2 8^4 / \|K_{SE}\|_{op}\}$. □